

Lipocalin-2 derived from adipose tissue mediates aldosterone-induced renal injury

Wai Yan Sun,^{1,2} Bo Bai,^{1,2} Cuiting Luo,^{1,2} Kangmin Yang,^{1,2} Dahui Li,^{1,2} Donghai Wu,³ Michel Félétou,⁴ Nicole Villeneuve,⁴ Yang Zhou,⁵ Junwei Yang,⁵ Aimin Xu,^{1,2} Paul M. Vanhoutte,^{1,2} and Yu Wang^{1,2}

¹The State Key Laboratory of Pharmaceutical Biotechnology and ²Department of Pharmacology and Pharmacy, The University of Hong Kong, Hong Kong SAR, China. ³Key Laboratory of Regenerative Biology, Guangzhou Institute of Biomedicine and Health, Chinese Academy of Sciences, Guangzhou, China. ⁴The Institut de Recherches Servier, Suresnes, France. ⁵Center for Kidney Disease, Second Affiliated Hospital, Nanjing Medical University, China.

Lipocalin-2 is not only a sensitive biomarker, but it also contributes to the pathogenesis of renal injuries. The present study demonstrates that adipose tissue-derived lipocalin-2 plays a critical role in causing both chronic and acute renal injuries. Four-week treatment with aldosterone and high salt after uninephrectomy (ANS) significantly increased both circulating and urinary lipocalin-2, and it induced glomerular and tubular injuries in kidneys of WT mice. Despite increased renal expression of *Lcn2* and urinary excretion of lipocalin-2, mice with selective deletion of *Lcn2* alleles in adipose tissue (Adipo-LKO) are protected from ANS- or aldosterone-induced renal injuries. By contrast, selective deletion of *Lcn2* alleles in kidney did not prevent aldosterone- or ANS-induced renal injuries. Transplantation of fat pads from WT donors increased the sensitivity of mice with complete deletion of *Lcn2* alleles (LKO) to aldosterone-induced renal injuries. Aldosterone promoted the urinary excretion of a human lipocalin-2 variant, R81E, in turn causing renal injuries in LKO mice. Chronic treatment with R81E triggered significant renal injuries in LKO, resembling those observed in WT mice following ANS challenge. Taken in conjunction, the present results demonstrate that lipocalin-2 derived from adipose tissue causes acute and chronic renal injuries, largely independent of local *Lcn2* expression in kidney.

Introduction

Without treatment, chronic kidney disease (CKD) progresses to end-stage renal failure (1). The renin-angiotensin-aldosterone system (RAAS) plays a critical role in causing vascular, inflammatory, and fibrotic damages during the development of renal dysfunction and insufficiency (2). Pharmacological inhibition of the renin-angiotensin system (RAS) ameliorates the progression of CKD in experimental animals and humans (3, 4). However, such blockade often leads to the overproduction of aldosterone and subsequent activation of mineralocorticoid receptor (MR) (5). Excessive aldosterone production induces glomerulosclerosis, tubular cell injury, and interstitial fibrosis, independently of changes in arterial blood pressure and volume homeostasis, thus contributing to the development of end-stage renal failure (6, 7). MR antagonists (e.g., spironolactone and eplerenone) slow the progression of CKD and decrease mortality in patients with hypertension, diabetic nephropathy, or congestive heart failure (8, 9). However, their use is limited by hyperkalemia (10).

Besides regulating electrolyte balance and blood volume, aldosterone modulates metabolism and energy homeostasis by acting on adipose tissues (11, 12). It stimulates the differentiation of white adipocytes and modulates the thermogenic capacity of brown fat (13, 14). In mice, aldosterone treatment does not alter the percentage of body fat mass but promotes the phenotypic switch of white and brown adipose tissues (15). In patients with primary aldosteronism, adiponectin expression is reduced in adipose tissue; in vitro studies demonstrate that aldosterone decreases the production of this adipokine in adipocytes (16, 17). MR expression is increased in adipose tissues of obese individuals and animals, facilitating the development of cardiometabolic syndrome and vascular dysfunction (18, 19). Systemic MR antagonism improves adipose tissue function and metabolic performance in mice with either genetic or dietary obesity (20, 21). To date, the relative importance of aldosterone and/or MR signaling in adipose tissue as a potential cause of renal dysfunction and CKD remains unknown.

Conflict of interest: The authors have declared that no conflict of interest exists.

Submitted: February 23, 2018

Accepted: July 24, 2018

Published: September 6, 2018

Reference information:

JCI Insight. 2018;3(17):e120196.

<https://doi.org/10.1172/jci.insight.120196>.

insight.120196.

Lipocalin-2 is a proinflammatory molecule upregulated in obese individuals or patients with cardio-metabolic syndrome (22–24). It was originally discovered as a granular protein from neutrophils (25). However, the mRNA of *lcn2* was not expressed in mature or tissue-infiltrating neutrophils (23, 26). In adipocytes, lipocalin-2 is expressed constitutively at both the gene and protein levels (22). In epithelial cells, lipocalin-2 is induced predominantly by involution, injury, or dysplastic transformation, and it modulates the phenotype of the epithelial lineage during growth and in disease (27). At the tissue level, lipocalin-2 expression is influenced by development, ageing, infection, and the inflammatory status (22, 26). For example, lipocalin-2 is undetectable or present at very low levels in heart and kidney under physiological conditions but significantly increased in response to injury, infection, or other pathological conditions (17, 28).

Lipocalin-2 is a sensitive, specific, and predictive early biomarker of acute kidney injury (AKI) (28). Both circulating and urinary levels of lipocalin-2 increase within a few hours after cardiopulmonary bypass surgery (28, 29). Augmented serum and urinary lipocalin-2 levels are associated with renal damages in CKD patients (30). Subjects with higher baseline lipocalin-2 levels exhibit an increased risk of CKD progression when compared with those with lower baseline values, even after adjustment for changes in glomerular filtration rate (GFR) (31). The ratio between urinary lipocalin-2 and creatinine is positively correlated with mortality in patients with CKD (32). The plasma concentration of lipocalin-2 increases progressively with the reduction of GFR, due to impaired removal of the protein from the circulation (33). At the end stage of renal failure, urinary levels of lipocalin-2 inversely correlate with the residual estimated GFR and microalbuminuria (32, 34).

In humans, circulating levels of lipocalin-2/matrix metalloproteinase 9 protein complexes are positively correlated with the plasma concentration of aldosterone (35), whereas urinary lipocalin-2 is positively correlated with the hormone in the urine (23). In animals, lipocalin-2 has been identified as a downstream target for aldosterone/MR in the cardiovascular system, kidney, and neutrophils (35, 36). It plays a key role in aldosterone/MR-mediated vascular fibrosis; deficiency of lipocalin-2 blunts aldosterone-induced hypertension and the associated elevation of fibrotic markers (35). Despite this information, the detailed role and the precise sources of lipocalin-2 in mediating aldosterone-induced renal injuries remain uncharacterized.

Obesity, hypertension, and type 2 diabetes are associated with an increased risk of CKD (37). Obesity is considered as a blood volume-independent stimulus for the overproduction of aldosterone (38). The plasma aldosterone concentration is positively correlated with the amount of visceral adipose tissue, which produces all RAAS components independently of systemic regulation (39). In view of the close relationship between CKD and obesity, the present study examined the hypothesis that aldosterone stimulates the production of lipocalin-2 by adipose tissues, in turn causing kidney damage and renal fibrosis. Mouse models with selective deletion of *lcn2* alleles in adipose tissue (Adipo-LKO) or kidney (Wt1^{CreERT2}-LKO or Wt1^{CreGFP}-LKO, referred to as Wt1-LKO) were used for the following investigations.

Results

ANS treatment induces lipocalin-2 expression in both kidney and adipose tissues. Under basal conditions, the serum and urinary lipocalin-2 levels were not significantly different between WT and Adipo-LKO mice (Figure 1A). At the age of 12 weeks, mice were subjected to uninephrectomy followed by chronic aldosterone/salt treatment (ANS). When compared with sham controls, 4-week ANS treatment significantly augmented the concentrations of lipocalin-2 in serum (~2-fold) and urine (over 6-fold) samples collected from WT mice (Figure 1A). In Adipo-LKO mice, ANS did not elevate the circulating levels (Figure 1A, left) but increased the urinary excretion of lipocalin-2 by ~2-fold (Figure 1, right). The amounts of lipocalin-2 in urine samples of ANS-treated Adipo-LKO were significantly lower than those of ANS-treated WT mice (Figure 1A, right). Four-week ANS treatment caused renomegaly and excessive urination in all groups of mice, although the kidney/body weight ratio and the 24-hour urine volume were significantly lower in ANS-treated LKO than those of ANS-treated WT or Adipo-LKO mice (Supplemental Figure 1; supplemental material available online with this article; <https://doi.org/10.1172/jci.insight.120196DS1>).

ANS treatment significantly increased the mRNA and protein levels of lipocalin-2 in kidney and epididymal adipose tissues of WT mice (Figure 1, B and C). The mRNA expression of *lcn2* was undetectable in epididymal adipose tissues but significantly upregulated by ANS treatment in kidneys of Adipo-LKO mice (Figure 1B). Results from in situ hybridization demonstrated that *lcn2* mRNA transcripts were induced by ANS in the distal tubules of kidneys of both WT and Adipo-LKO mice (Supplemental Figure 2). The protein levels of lipocalin-2 in kidneys of Adipo-LKO mice were also increased by ANS but remained

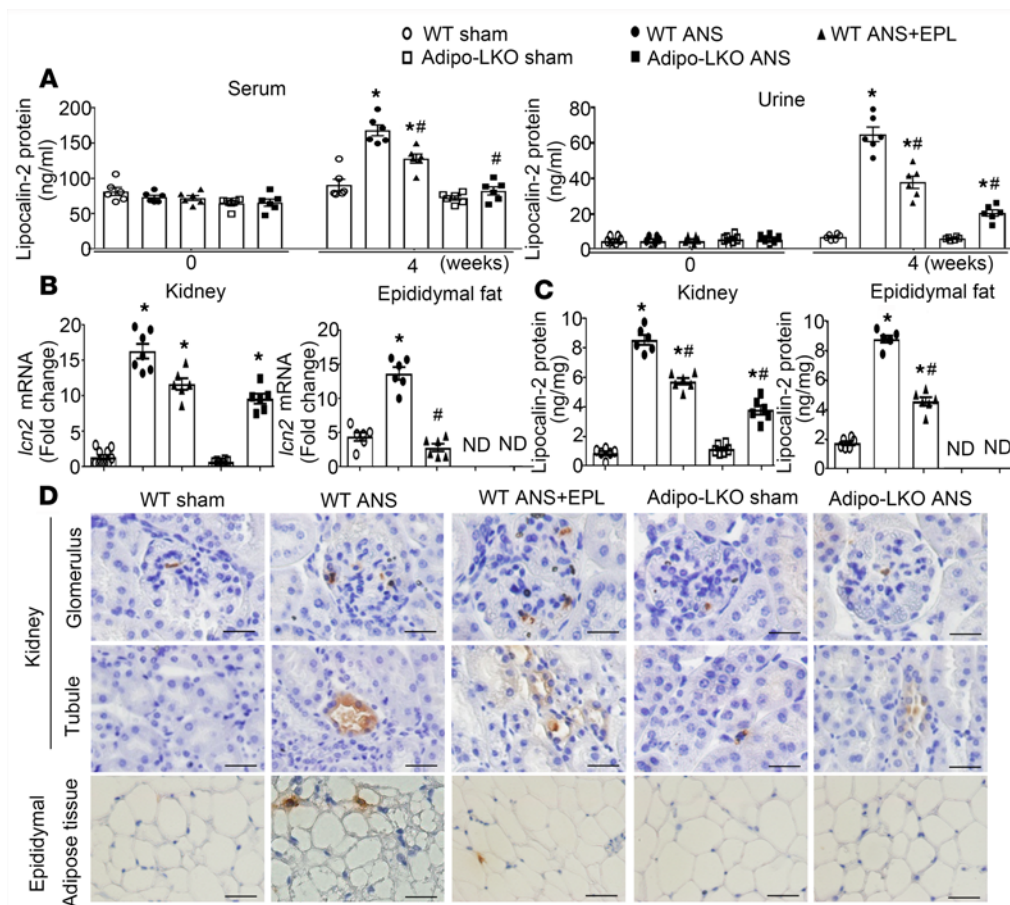


Figure 1. WT mice treated with ANS (uninephrectomy, aldosterone 200 $\mu\text{g}/\text{kg}/\text{day}$, salt 1%) exhibited increased lipocalin-2 expressions in kidney and adipose tissues. (A) WT and Adipo-LKO mice (12 weeks old) were subjected to sham or 4-week ANS treatment. Eplerenone (EPL) was given to the WT mice 1 week after starting the ANS treatment and continued for another 3 weeks. Serum and urine samples were collected before and after the treatment for measuring lipocalin-2 levels by ELISA. (B and C) The mRNA expression of *lcn2* and the protein content of lipocalin-2 were examined in kidney and epididymal adipose tissue by qPCR (B) and ELISA (C). (D) The localization of lipocalin-2 protein in kidney and adipose tissue sections was examined by IHC using an antibody specifically recognizing murine lipocalin-2. Magnification, 400 \times . Scale bars: 20 μm . Data are presented as mean \pm SEM; * $P < 0.05$ vs. WT sham controls; # $P < 0.05$ vs. WT ANS by ANOVA with the Bonferroni *post hoc* test ($n = 6-8$).

significantly lower than those of WT mice undergoing the same treatment (Figure 1C, left). In contrast to ANS-treated WT, the protein contents of lipocalin-2 were undetectable in adipose tissues of ANS-treated Adipo-LKO mice (Figure 1C, right). Immunohistochemical analyses revealed that lipocalin-2 protein was present in the glomeruli and proximal tubules of kidneys collected from ANS-treated WT mice but was significantly reduced in those of ANS-treated Adipo-LKO mice (Figure 1D and Supplemental Figure 1B). Cells positively stained with lipocalin-2 protein were present in adipose tissues from ANS-treated WT but were absent in those of Adipo-LKO mice (Figure 1D and Supplemental Figure 1B).

Three-week eplerenone treatment significantly reduced the circulating and urinary levels of lipocalin-2 (Figure 1A), downregulated its mRNA and protein expressions in adipose tissues (Figure 1, B–D), but had no significant effects on *lcn2* gene transcription in kidneys of ANS-treated WT animals (Figure 1B and Supplemental Figure 2). Moreover, eplerenone prevented ANS-induced adipose expression of genes involved in steroid metabolism and signaling, such as *nr3c2* (MR), *nr3c1* (glucocorticoid receptor), *hsd3b1* (3 β -hydroxysteroid dehydrogenase type 1) and *cyp21a1* (cytochrome P450, family 21, subfamily a, polypeptide 1), to similar extents as those of Adipo-LKO and LKO mice (Supplemental Figure 3).

The results demonstrate that, while ANS treatment significantly induced lipocalin-2 expression in both kidneys and adipose tissues of WT mice, blocking MR with eplerenone mainly attenuated *lcn2* expression in the latter, thus reducing the circulating levels and urinary excretion of this protein. Deletion of *lcn2* alleles selectively in adipose tissue significantly reduced the amount of lipocalin-2 in the

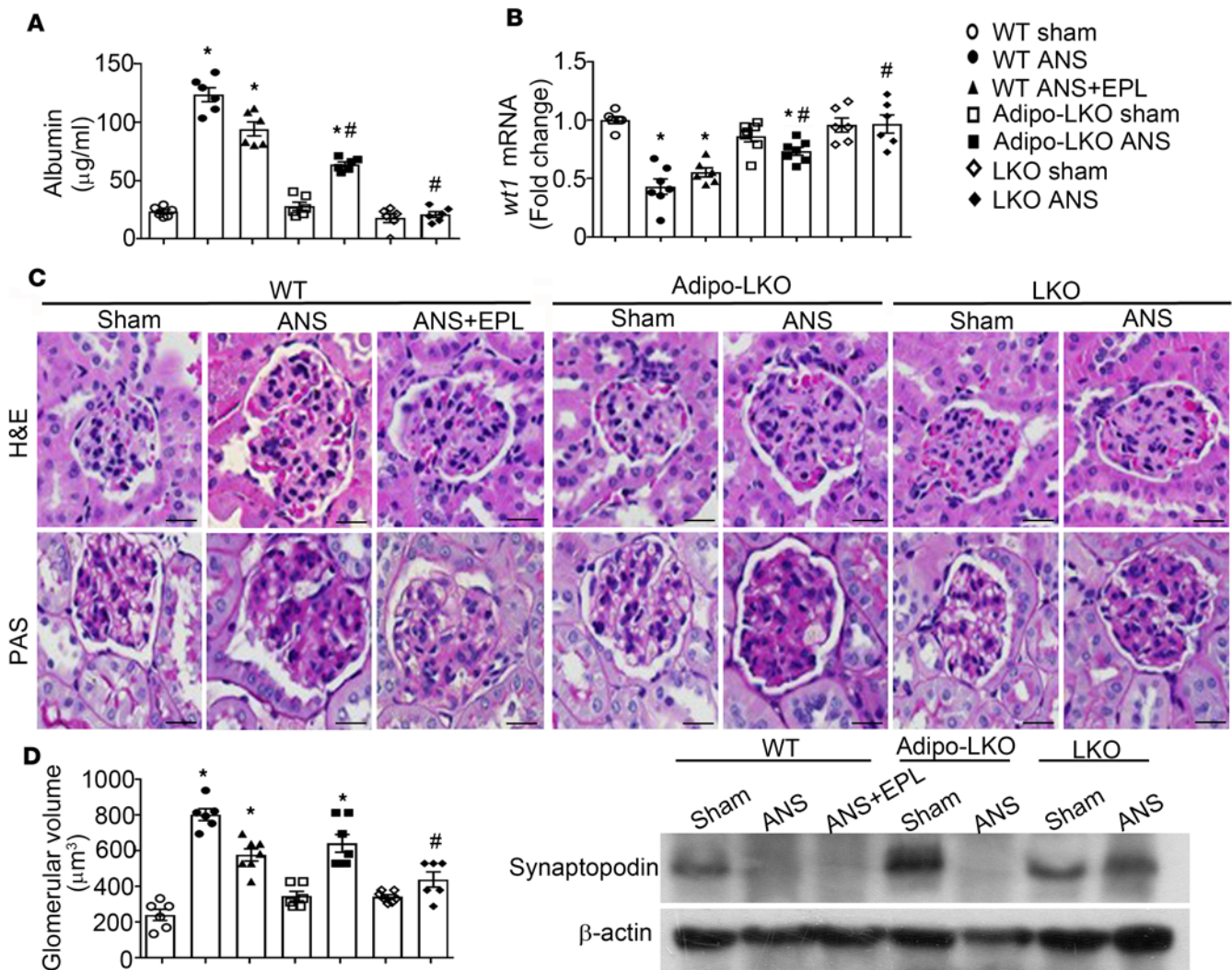


Figure 2. Deficiency of lipocalin-2 protects mice from ANS-induced glomerular injuries in the kidney. (A) WT, Adipo-LKO, and LKO mice were subjected to sham or 4-week ANS challenge as in Figure 1. At the end of treatment, urine samples were collected for measuring albumin levels as described in Methods. (B) The mRNA expression of *wt1* in kidney was evaluated by qPCR and presented as fold changes against WT sham controls. (C) Morphology of the glomeruli was examined in kidney tissue sections by both H&E (upper row) and PAS (lower row) staining. Magnification, 400 \times . Scale bar: 20 μm . (D) The glomerular area was quantified using ImageJ software and expressed as glomerular volume (D, left). The protein levels of synaptopodin were determined by Western blotting using the tissue lysates prepared from kidney samples (D, right). Data are shown as mean \pm SEM; * P < 0.05 vs. corresponding sham controls; # P < 0.05 vs. WT ANS by Mann-Whitney nonparametric Student's *t* test (n = 6–8). EPL, eplerenone.

circulation, kidney, and urine samples of ANS-treated animals. Taken in conjunction, these data indicate a role of adipose tissue–derived lipocalin-2 in aldosterone-induced renal pathologies.

Selective lipocalin-2 depletion in adipose tissue attenuates ANS-induced renal injuries. Prolonged hyperaldosteronism causes hypertension and organ damages (17). Four-week ANS treatment significantly increased the systolic arterial blood pressure of WT but not that of Adipo-LKO and LKO mice (Supplemental Figure 4). Eplerenone significantly reduced the systolic blood pressure in ANS-treated WT mice to a level similar to that of Adipo-LKO and LKO mice. Albumin excretion was measured in the 24-hour urine samples collected from sham- or ANS-treated animals. Microalbuminuria appeared in ANS-treated WT and Adipo-LKO but not in LKO mice (Figure 2A). The mRNA expressions of Wilms tumor 1 (*wt1*), a key transcription factor regulating podocyte function (40), were significantly downregulated by ANS in kidneys of WT and Adipo-LKO mice (Figure 2B). By contrast, the mRNA levels of *wt1* did not differ significantly between sham- and ANS-treated LKO mice (Figure 2B). Eplerenone had little effects on ANS-induced microalbuminuria and did not prevent the downregulation of *wt1* in ANS-treated WT kidneys (Figure 2, A and B).

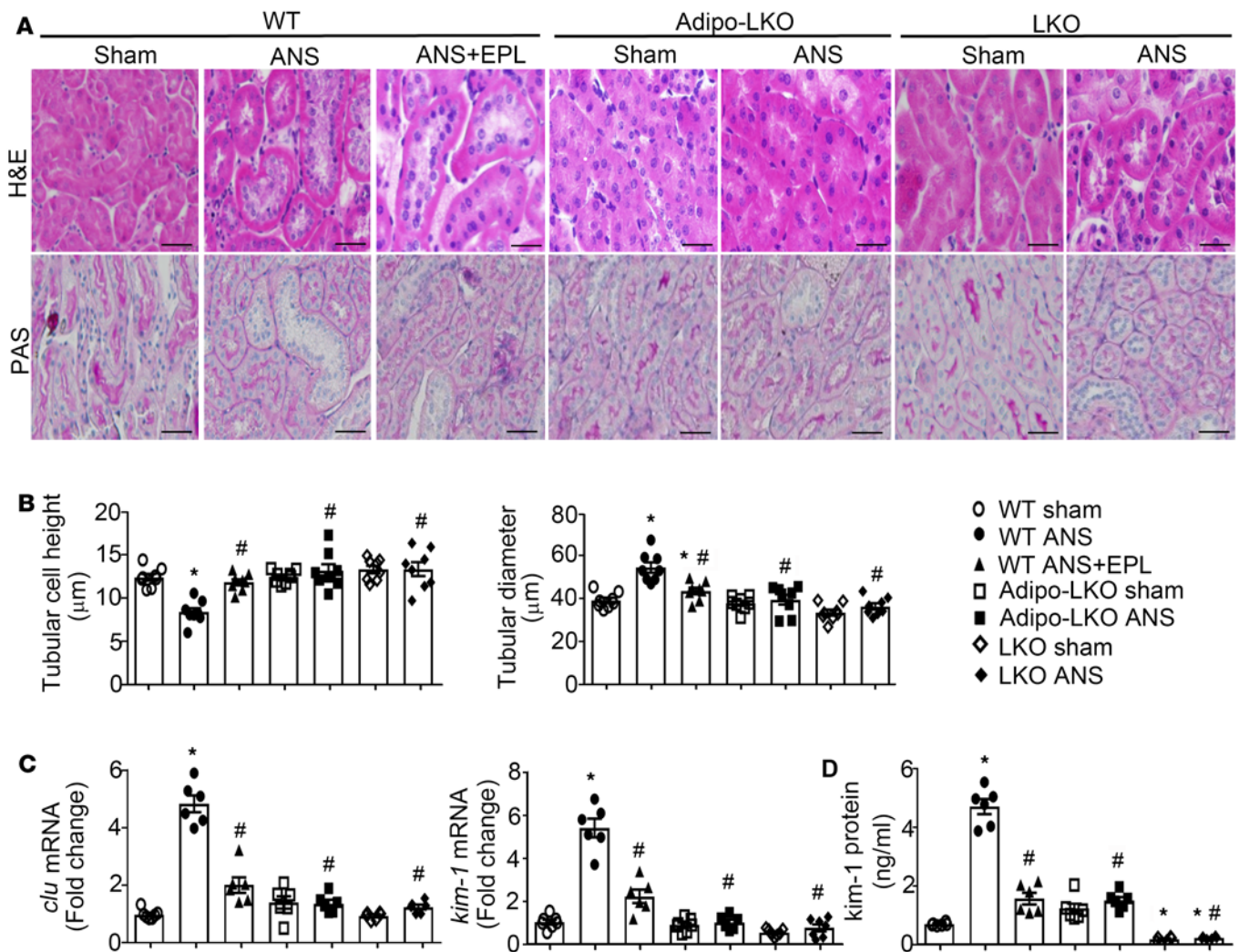


Figure 3. Deficiency of lipocalin-2 protects mice from ANS-induced tubular injuries in the kidney. (A) WT, Adipo-LKO, and LKO mice were subjected to sham or ANS treatment as in Figure 1. Morphological changes of renal tubules were examined by H&E (upper row) or PAS (lower row) staining. Images of proximal tubules in the cortex are shown. Magnification, 400 \times . Scale bar: 20 μ m. (B) Quantification of tubular cell height and diameter was performed using ImageJ software. (C) Ten random images from 1 animal were examined to calculate the average data for comparison. The mRNA expression levels of *clu* and *kim-1* in kidney samples were measured by qPCR and presented as fold changes against WT sham controls. (D) The protein amount of Kim-1 in the 24-hour urine samples was measured by ELISA for comparison. Data are shown as mean \pm SEM; * P < 0.05 vs. WT sham controls; # P < 0.05 vs. WT ANS by Mann-Whitney nonparametric Student's t test (n = 6–8). EPL, Eplerenone.

H&E and Periodic Acid-Schiff (PAS) staining were performed to evaluate glomerular morphology (Figure 2C). ANS significantly increased the glomerular volume in kidneys of WT ($786 \pm 102 \mu\text{m}^3$ vs. $317 \pm 18 \mu\text{m}^3$ in WT sham controls, P < 0.05) and Adipo-LKO ($630 \pm 129 \mu\text{m}^3$ vs. $346 \pm 69 \mu\text{m}^3$ in Adipo-LKO sham control, P < 0.05) mice (Figure 2D, left). Depletion of lipocalin-2 expression prevented the enlargement of glomeruli in ANS-treated LKO mice ($430 \pm 102 \mu\text{m}^3$ vs. $348 \pm 26 \mu\text{m}^3$ in LKO sham controls). Western blotting revealed that the protein expression of synaptopodin, a podocyte foot-process protein (41), was down-regulated by ANS in kidneys of WT and Adipo-LKO but not LKO animals (Figure 2D, right).

H&E and PAS staining were performed to evaluate tubular injuries. When compared with sham controls, significant changes in the morphology were observed in ANS-treated WT kidneys, including dilatation of tubules, epithelial swelling and flattening, as well as brush border loss (Figure 3A). Quantitative analyses revealed that ANS-treated WT mice exhibited a reduced tubular cell height and an increased tubular diameter (Figure 3B). ANS-induced changes in tubular structure were largely prevented by lipocalin-2 deficiency in both Adipo-LKO and LKO mice (Figure 3, A and B). The renal expressions of *clu* (clusterin) and *kim-1* (kidney injury molecule-1), 2 indicators of tubular injury (42), were augmented significantly by

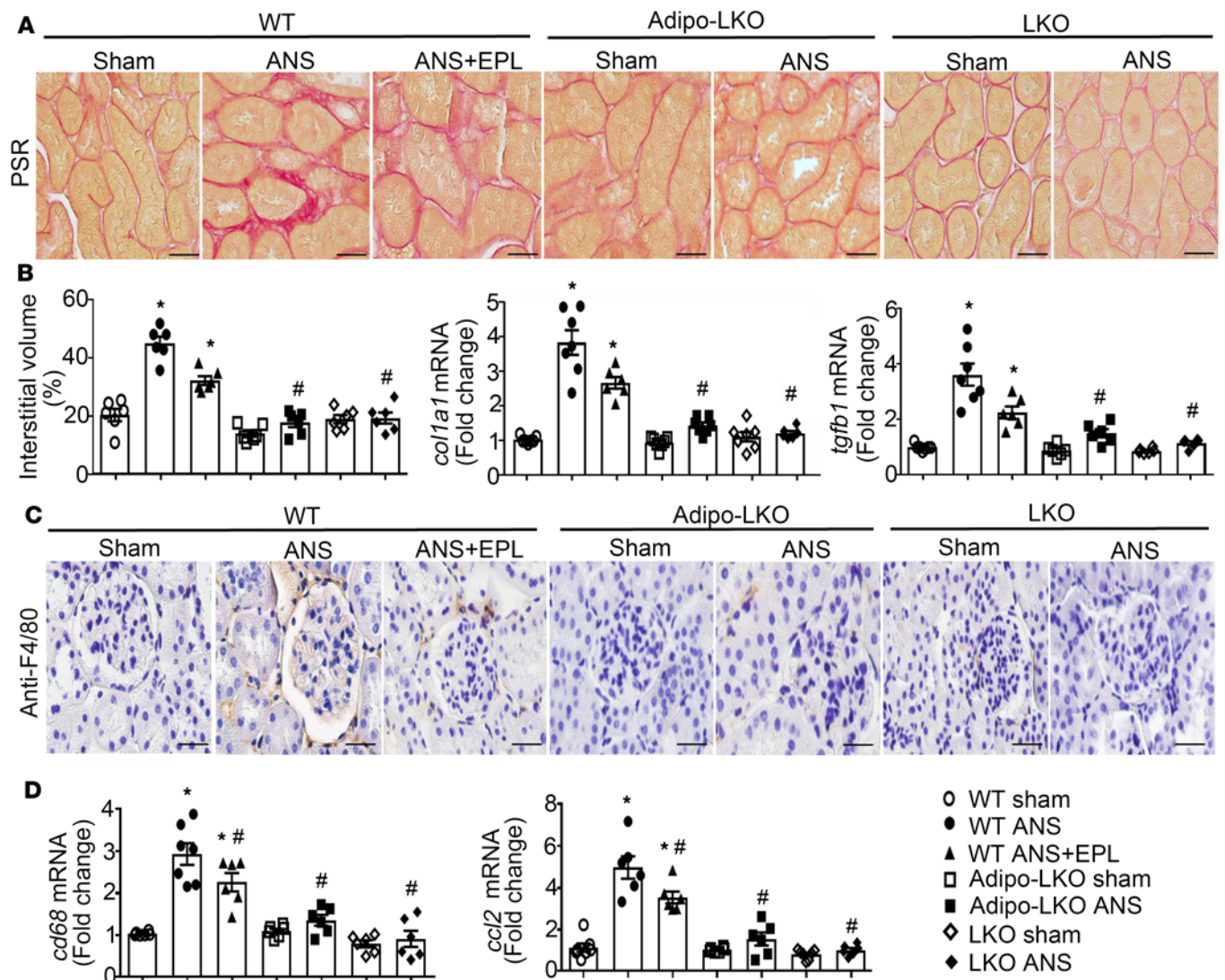


Figure 4. Deficiency of lipocalin-2 protects mice from ANS-induced interstitial fibrosis and macrophage infiltration in the kidney. (A) After sham or ANS treatment as in Figure 1, kidney tissue sections were prepared from WT, Adipo-LKO, and LKO mice. PSR staining was performed to examine fibrotic renal damage. Magnification, 400 \times . Scale bar: 20 μ m. (B) ImageJ software was used to quantify the interstitial volume. Ten random images from 1 animal were examined to calculate the percentage values (B, left). The mRNA expression levels of *col1a1* and *tgfb1* in kidney tissues were examined by qPCR and shown as fold changes against WT sham controls (B, middle and right). (C) Macrophage infiltration was evaluated in kidney tissue sections by IHC staining using an antibody recognizing F4/80. Magnification, 400 \times . Scale bar: 20 μ m. (D) The mRNA expression levels of *cd68* and *ccl2* in kidney tissues were examined by qPCR and presented as fold changes against WT sham controls. Data are shown as mean \pm SEM; * P < 0.05 vs. WT sham controls; # P < 0.05 vs. WT ANS by Mann-Whitney nonparametric Student's t test (n = 6–8). EPL, eplerenone.

ANS in kidneys of WT mice (Figure 3C). The amount of Kim-1 protein was also significantly elevated in the urine samples of ANS-treated WT animals (Figure 3D). Eplerenone treatment, as well as lipocalin-2 deficiency, significantly prevented the upregulation of *clu* and *kim-1* in kidneys and Kim-1 in urine samples of ANS-treated WT, Adipo-LKO, and LKO mice, respectively (Figure 3, C and D).

Picrosirius red (PSR) staining was performed to evaluate tubulointerstitial fibrosis (Figure 4A). ANS treatment significantly increased the interstitial volume in kidneys of WT but not in those of Adipo-LKO and LKO mice (Figure 4B, left). Consistently, the mRNA levels of the fibrotic markers, including *col1a1* (collagen type I, alpha 1) and *tgfb1* (transforming growth factor β 1), were upregulated significantly by ANS in kidneys of WT but not in those of Adipo-LKO and LKO mice (Figure 4B, middle and right). Furthermore, ANS-induced macrophage infiltration and gene expressions of *cd68* (cluster of differentiation 68) and *ccl2* (monocyte chemoattractant protein-1) were prevented by lipocalin-2 deficiency in both Adipo-LKO and LKO mice (Figure 4, C and D). Administering eplerenone decreased the interstitial volume and expression

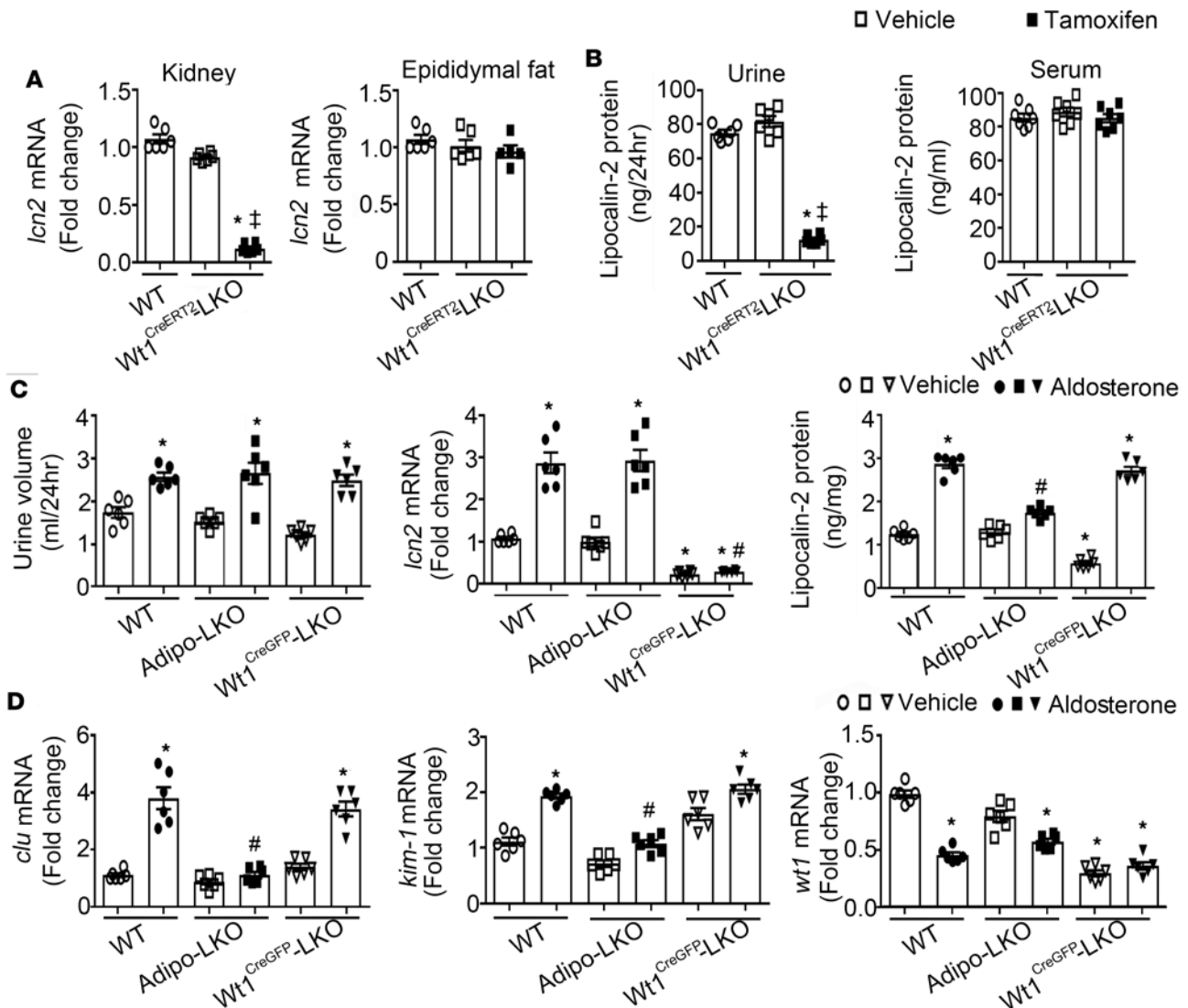


Figure 5. Lipocalin-2 of nonkidney source mediated aldosterone-induced acute renal injuries. (A) $Wt1^{CreERT2}$ -LKO mice were treated with vehicle or tamoxifen (33 mg/kg/day, i.p. injection for 5 days). After treatment, *lcn2* expressions in kidney and epididymal adipose tissue were examined by qPCR and presented as fold changes against WT controls. (B) The 24-hour urine and serum samples were collected to measure lipocalin-2 levels by ELISA. (C) WT, Adipo-LKO, and $Wt1^{CreGFP}$ -LKO mice were injected with 1 dose of either vehicle or aldosterone (2 mg/kg; s.c.) as described in the Methods. The 24-hour urine samples were collected to compare urination (C, left). qPCR and ELISA were performed to measure the mRNA expressions of *lcn2* and protein amounts of lipocalin-2 in kidney (C, middle and right). (D) Renal injury markers, including *clu*, *kim-1*, and *wt1* were examined by qPCR and presented as fold changes against the WT vehicle controls. Data are shown as mean \pm SEM; * $P < 0.05$ vs. WT vehicle groups; # $P < 0.05$ vs. $Wt1^{CreERT2}$ -LKO with vehicle treatment; * $P < 0.05$ vs. WT treated with aldosterone by Mann-Whitney nonparametric Student's *t* test ($n = 6$).

of fibrotic parameters in ANS-treated WT kidneys (Figure 4, A and B) and significantly reduced the number of infiltrated macrophages, as well as the expression of inflammatory genes (Figure 4, C and D).

In summary, the above results demonstrated that selective deletion of *lcn2* alleles in adipose tissue was as effective as complete depletion of lipocalin-2 expression to protect mice against ANS-induced tubular and interstitial lesions, especially the fibrotic and inflammatory damages. However, adipose tissue deletion of *lcn2* alleles was less protective than complete deficiency of lipocalin-2 against ANS-induced microalbuminuria and glomerulopathy, indicating that the production of this molecule from other sources contributed to the glomerular damages in ANS-treated animals.

Adipose tissue-derived lipocalin-2 mediates aldosterone- or ANS-induced renal injuries. Mice with a mutation of *wt1* exhibit glomerular injury and proteinuric nephropathies; lipocalin-2 deficiency does not affect the glomerular lesions but significantly attenuates tubular injuries in these animals (43). As *wt1* was abundantly expressed in kidney (data not shown), $Wt1$ -LKO mice were established to selectively delete *lcn2* alleles in

Wt1-expressing cells without disrupting the *wt1* functions. In Wt1^{CreERT2}-LKO mice, tamoxifen treatment (33 mg/kg/day i.p. for 5 days) significantly reduced the kidney expressions of *lcn2* and urinary excretion of lipocalin-2 by over 80%, but it did not cause significant changes of *lcn2* expression in epididymal adipose tissues and the circulating concentrations of this protein (Figure 5, A and B). These results indicated that, under basal conditions, urinary lipocalin-2 is mainly derived from Wt1-expressing cells in the kidney.

Next, WT, Adipo-LKO, and Wt1^{CreGFP}-LKO mice with selective deletion of *lcn2* alleles in kidney were treated acutely with vehicle or aldosterone (2 mg/kg). Urination was not significantly different in vehicle controls but increased by aldosterone in all 3 groups of mice (Figure 5C, left). The kidney tissues and 24-hour urine samples were collected to measure *lcn2* expression and lipocalin-2 protein levels. The basal *lcn2* mRNA and lipocalin-2 protein levels were significantly decreased in kidneys of Wt1^{CreGFP}-LKO, compared with those of WT and Adipo-LKO mice (Figure 5C, middle and right). Aldosterone treatment significantly augmented (more than 3-fold) the mRNA expressions of *lcn2* in kidneys of WT and Adipo-LKO mice, as well as the lipocalin-2 protein content in kidneys of WT and Wt1^{CreGFP}-LKO mice (Figure 5C, middle and right). Consistent with the elevated lipocalin-2 levels, the mRNA expressions of *clu* and *kim-1* were significantly upregulated by aldosterone in kidneys of WT and Wt1^{CreGFP}-LKO mice (Figure 5D, left and middle). Acute treatment with aldosterone did not increase the lipocalin-2 protein or the expression levels of tubular injury markers in kidneys of Adipo-LKO mice (Figure 5, C and D). The mRNA expression of *wt1* was significantly downregulated by aldosterone in kidneys of WT and Adipo-LKO mice, whereas the reduced expression of *wt1* in those of Wt1^{CreGFP}-LKO mice did not change after the acute treatment (Figure 5D, right).

Chronic ANS treatment was applied to Wt1^{CreGFP}-LKO mice with selective depletion of lipocalin-2 expressions in kidney. Four-week treatment with ANS did not change *lcn2* mRNA levels in the kidney but significantly augmented those in epididymal adipose tissues (Figure 6A, left). The *lcn2* mRNA expression was barely detectable in s.c. fat pads of these animals (Figure 6A, left). After ANS treatment, the protein levels of lipocalin-2 were significantly augmented in both kidney and epididymal adipose tissues of Wt1^{CreGFP}-LKO mice (Figure 6A, middle and right). When compared with WT, Adipo-LKO and LKO (Supplemental Figure 1), ANS treatment caused more severe renomegaly in Wt1^{CreGFP}-LKO mice (Figure 6B). Compared with WT mice, Wt1^{CreGFP}-LKO exhibited similar increases in the glomerular volume and alterations in tubular morphology and structure after ANS treatment (Figure 6C vs. Figure 2D and Figure 3B). The mRNA expressions of *clu*, *kim-1*, *cd68*, and *ccl2* were all significantly upregulated in kidneys of ANS-treated Wt1^{CreGFP}-LKO mice (Figure 6D). Compared with ANS-treated WT mice, the interstitial volume and mRNA expressions of *colla1* and *tgfb1* were increased by ANS but to a lower level in kidneys of Wt1^{CreGFP}-LKO mice (Supplemental Figure 5).

To further confirm that adipose tissue-derived lipocalin-2 contributed to aldosterone-induced renal injuries, fat transplantation was performed in LKO mice receiving the epididymal and s.c. adipose tissues from age- and sex-matched WT animals (Supplemental Figure 6). After 6 weeks of tissue transplantation, lipocalin-2 could be detected in both serum and urine samples of the LKO recipients (Supplemental Figure 6A, left). Acute aldosterone treatment enhanced the urinary excretion of this molecule (Supplemental Figure 6A, right). The *lcn2* mRNA expression was significantly augmented by aldosterone in the transplanted epididymal adipose tissues (Supplemental Figure 6B). The mRNA expression of *lcn2* in s.c. adipose tissues was more than 18-fold lower than that of epididymal adipose tissues. In kidneys of the recipient LKO mice, the mRNA expressions of *clu*, *kim-1*, *cd68*, and *ccl2* were all significantly upregulated by aldosterone treatment (Supplemental Figure 6C).

Collectively, the above data suggest that, while aldosterone or ANS induced *lcn2* expression and lipocalin-2 production in both kidney and adipose tissues, the latter represented a major source of the pathological form of lipocalin-2 to cause acute and chronic renal injuries largely independent of the local gene expression of this molecule. Aldosterone promoted the urinary excretion of the pathological form of lipocalin-2 from adipose tissues.

Treatment with lipocalin-2 variant R81E causes acute and chronic renal injuries. Lipocalin-2 is dynamically regulated by posttranslational modifications, ligand-binding, and/or protein-interactions in a tissue-specific manner (27, 36, 44–46). To evaluate the role of urinary excretion of lipocalin-2 in causing the acute and chronic renal injuries, LKO mice were subjected to treatment with different recombinant protein variants, without or with coadministering aldosterone. To this end, WT human lipocalin-2 (hLcn2) (22), C87A (a variant mimicking the nonpolyaminated human lipocalin-2; ref. 23, 44), or the iron-scavenging mutants with arginine 81 (R81E), lysine 125 (K125E), or lysine 134 (K134E) replaced by glutamic acid (47) were

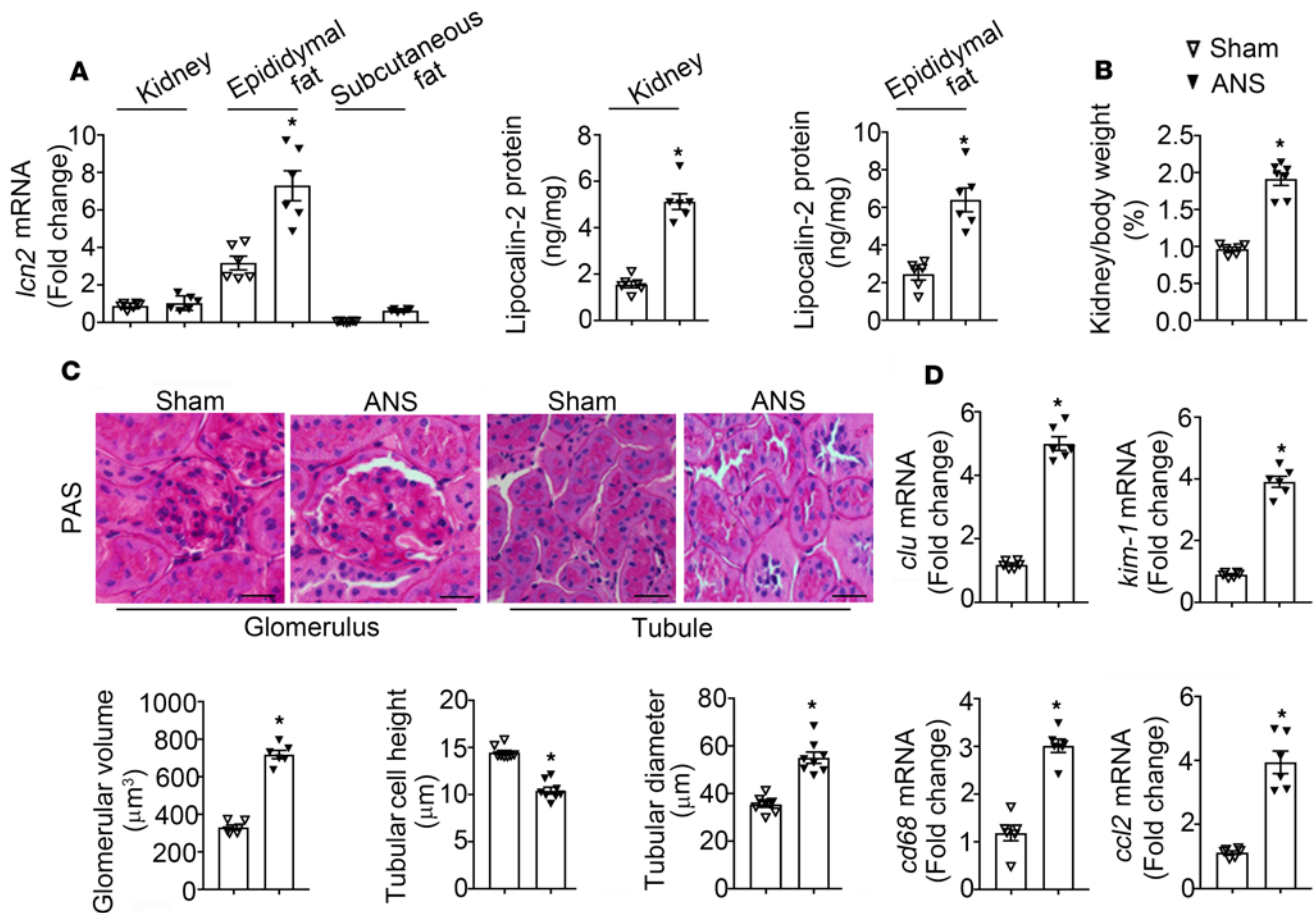


Figure 6. ANS treatment caused chronic renal injuries in mice with selective deletion of *lcn2* alleles in kidney. (A) $Wt1^{CreGFP-LKO}$ mice were subjected to sham or ANS treatment as in Figure 1. Kidney, epididymal, and s.c. adipose tissues were collected after 4-week treatment. qPCR was performed to measure the *lcn2* mRNA levels. The results are shown as fold changes against kidney samples of the sham control animals (A, left). ELISA was applied to examine the lipocalin-2 protein contents in kidney and epididymal adipose tissues (A, middle and right). (B) The wet weights of each kidney were recorded and calculated as percentage ratios against body weight for comparison. (C) PAS staining was used to evaluate the glomerular and tubular injuries in kidney of sham- or ANS-treated $Wt1^{CreGFP-LKO}$ mice (C, top). Magnification, 400 \times . Scale bar: 20 μm . The glomerular area, tubular cell height, and diameter were quantified by ImageJ software as described in Methods (C, bottom). (D) The gene expression levels of injury markers, including *clu*, *kim-1*, *cd68*, and *ccl2* were examined by qPCR and presented as fold changes against the sham controls. Data are shown as mean \pm SEM; * $P < 0.05$ vs. sham controls by Mann-Whitney nonparametric Student's *t* test ($n = 6$).

administered at a dose of 10 $\mu\text{g}/\text{mouse}$ immediately after vehicle or aldosterone. Urine samples were collected during the following 24 hours, prior to serum and tissue collections.

Without coadministering aldosterone, LKO mice receiving different recombinant proteins exhibited similar levels of human lipocalin-2 in their serum (~ 35 ng/ml) and 24-hour urine (less than 10 ng) samples (Figure 7A). Aldosterone treatment significantly increased the circulating levels of hLcn2, C87A, K125E, and K134E, except for R81E (Figure 7A, left), the levels of which were significantly augmented by ~ 4 -fold only in urine samples (Figure 7A, right). In line with the highest levels of human lipocalin-2 in their urine samples, the expressions of *clu* and *kim-1* were significantly upregulated in kidneys of LKO mice receiving R81E plus aldosterone (Figure 7B). Next, LKO mice were subjected to chronic treatment with vehicle, hLcn2, C87A, R81E, or K134E (10 $\mu\text{g}/\text{day}/\text{mouse}$; i.p. injection for 4 weeks), without coadministering aldosterone. At the end of treatment, kidneys were collected for evaluation. Compared with other types of human lipocalin-2, R81E significantly augmented the mRNA expressions of *clu*, *kim-1*, *cd68*, and *ccl2* in kidneys of LKO mice (Figure 7C). Kidney section of LKO mice treated with R81E exhibited significantly increased interstitial volume (Supplemental Figure 7) and the renal expressions of the fibrotic markers *colla1* and *tgfb1* (Figure 7D, left). In addition, the gene expression of *hsd3b1* was significantly upregulated in kidneys from R81E-treated LKO mice, accompanied by a significant elevation of urinary aldosterone levels (Figure 7D, right).

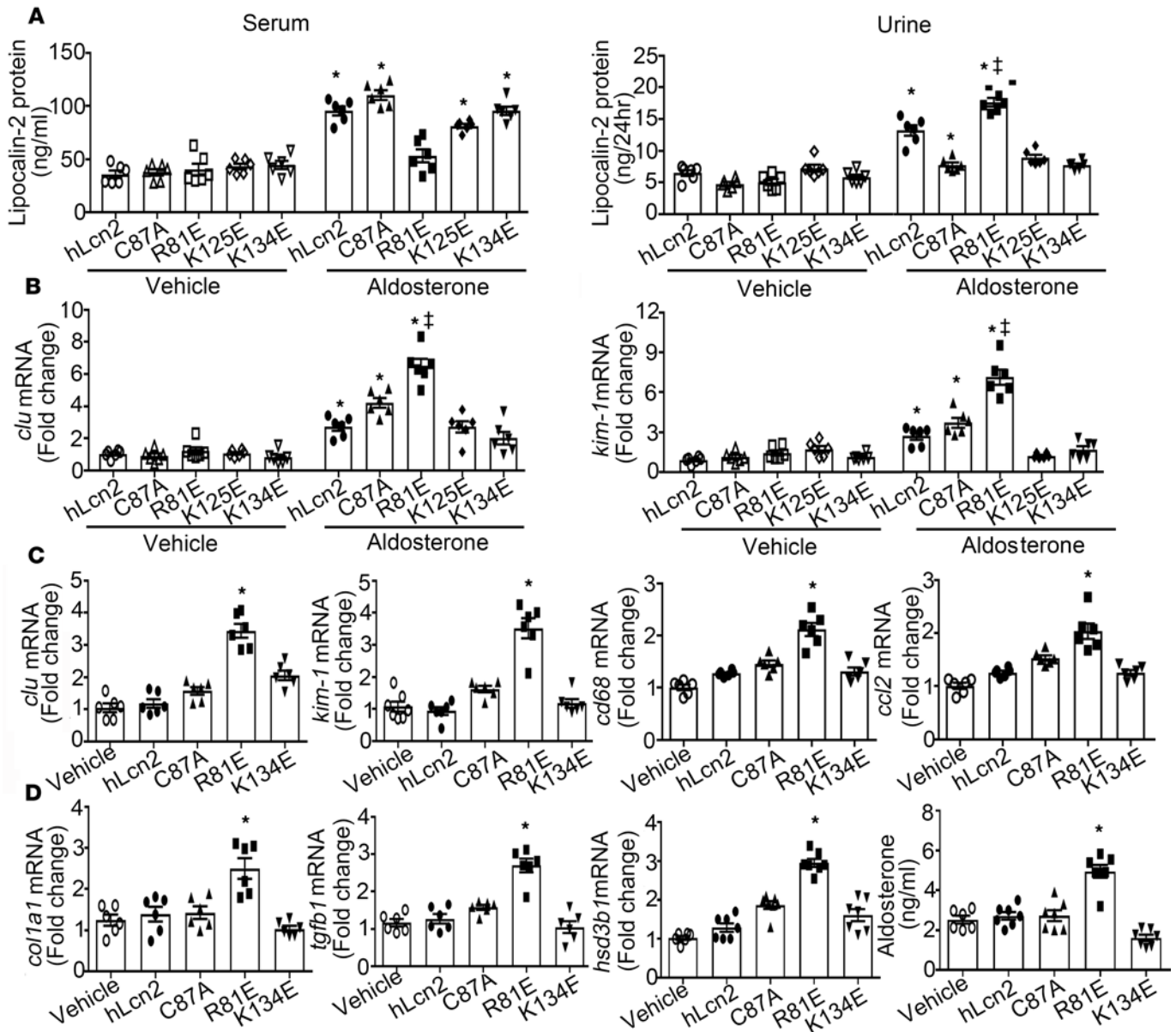


Figure 7. Acute or chronic treatment with recombinant proteins of human lipocalin-2 caused renal injuries in LKO mice. (A) LKO mice were administered with vehicle or aldosterone (2 mg/kg; s.c.), followed by an i.p. injection with 1 type of the recombinant human lipocalin-2 proteins (10 μ g/mouse), including hLcn2, C87A, R81E, K125E, or K134E. After 24 hours, the lipocalin-2 protein amount was examined in both serum and 24-hour urine samples by ELISA. (B) The kidney tissues were collected for qPCR to examine the mRNA expressions of *clu* and *kim-1*. Fold changes were calculated for comparison. (C and D) Chronic treatment was performed by i.p. injection with vehicle or 1 type of the recombinant human lipocalin-2 proteins (10 μ g/mouse/day), including hLcn2, C87A, R81E, and K134E. After 4-week treatment, kidney tissues were collected and subjected to qPCR for measuring the mRNA expressions of gene markers for cellular (*clu* and *kim-1*) and inflammatory (*cd68* and *ccl2*) injuries (C), or fibrotic tissue damages (*col1a1* and *tgfb1*) (D, left). The mRNA expression of steroid biosynthesis enzyme *hsc3b1* was measured by qPCR and the aldosterone concentrations in urine samples were measured by ELISA (D, right). Data are shown as mean \pm SEM; * P < 0.05 vs. corresponding vehicle groups; # P < 0.05 vs. hLcn2 aldosterone group by Mann-Whitney nonparametric Student's *t* test (n = 6–8).

A sandwich ELISA was developed to selectively detect the R81E form of lipocalin-2 in 100 human samples collected from the Hong Kong healthy volunteer cohort (23). In contrast to the other 2 forms of human lipocalin-2, hLcn2 and C87A (23), the plasma and urine R81E levels did not exhibit significant differences between male and female subjects (Table 1). After adjustment with age, smoking, and BMI, the urine R81E and the ratio of urine/plasma R81E were both positively correlated with biomarkers for kidney injury, including Kim-1 and haptoglobin, and negatively correlated with biomarkers for glomerular filtration, including serum cystatin C, plasma creatinine, and albumin-to-creatinine ratio (ACR). There was also a positive correlation between aldosterone and R81E levels in the urine (Table 1).

Table 1. Correlations between urine/plasma lipocalin-2 concentrations and study variables of Hong Kong healthy volunteer cohort.

	Total cohort (n = 100)	Male (n = 59)	Female (n = 41)	Urine R81E ^A				Plasma R81E				Urine/Plasma R81E ^A			
				r ^B	r ^C	P ^B	P ^C	r ^B	r ^C	P ^B	P ^C	r ^B	r ^C	P ^B	P ^C
Urine R81E (ng/ml)	3.92 (1.74–8.78)	3.48 (1.57–7.21)	5.64 (1.95–13.49)	/	/	/	/	/	/	/	/	/	/	/	/
Plasma R81E (ng/ml)	39.0 (31.8–48.1)	39.2 (33.8–46.5)	35.3 (30.5–49.9)	/	/	/	/	/	/	/	/	/	/	/	/
Urine/plasma R81E	0.10 (0.02–0.23)	0.09 (0.04–0.18)	0.16 (0.01–0.33)	/	/	/	/	/	/	/	/	/	/	/	/
Urine Kim-1 (ng/ml)	0.15 (0.02–0.47)	0.26 (0.02–0.66)	0.10 (0.01–0.25)	0.355	0.357	0.001	0.001	-	-	-	-	0.306	0.308	0.003	0.003
Urine aldosterone ^A (ng/ml)	1.009 (0.482–2.013)	1.441 (0.596–2.640)	0.962 (0.423–1.598)	0.341	0.345	0.001	0.001	-	-	-	-	0.323	0.331	0.002	0.001
Urine haptoglobin ^A (ng/ml)	6.3 (6.2–17.9)	6.3 (6.2–17.8)	6.4 (6.3–28.0)	0.189	0.190	0.046	0.046	-	-	-	-	0.187	0.190	0.048	0.047
Serum cystatin C (mg/ml)	0.26 (0.14–0.33)	0.31 (0.21–0.40)	0.19 (0.10–0.27)	-0.242	-0.238	0.015	0.017	-	-	-	-	-0.228	-	0.021	-
Urine albumin (μg/ml)	11.1 (5.2–18.4)	10.1 (3.9–17.7)	12.3 (6.3–20.0)	-0.374	-0.377	<0.001	<0.001	-	-	-	-	-0.355	-0.361	0.001	0.001
Plasma creatinine (μmol/l)	51.1 (45.5–58.3)	53.1 (49.2–60.3)	46.5 (43.3–54.1)	-0.303	-0.301	0.003	0.019	-	-	-	-	-0.317	-0.314	0.002	0.002
Urinary Creatinine (mmol/l)	5.0 (2.5–12.2)	6.4 (3.5–15.2)	3.5 (1.5–7.9)	0.328	0.211	0.001	0.030	-	-	-	-	0.337	0.353	0.001	0.001
ACR, mg/mmol ^A	2.3 (0.5–5.4)	1.5 (0.3–5.1)	4.1 (1.2–8.6)	-0.251	-0.257	0.012	0.011	-	-	-	-	-0.228	-0.240	0.021	0.016

Data were shown as median (interquartile range). ^A Logarithmic transformed before analyses. ^B Adjustment with age and smoking. ^C Adjustment with age, smoking and BMI.

These results demonstrate that, under various pathophysiological conditions, certain forms of human lipocalin-2 derived from nonkidney sources cause tubular, fibrotic, and inflammatory injuries in the kidney. Thus, chronic elevation of the pathological forms of lipocalin-2, such as those produced in adipose tissue, contributed to the pathogenesis of CKD, largely independent of the local *lcn2* expressions in the kidney (Figure 8).

Discussion

Increased production of aldosterone and the activation of MR contribute to the development of CKD not only by increasing sodium retention and potassium loss, but also by causing tissue fibrosis and vascular damage (48–52). The renal protective effects of MR inhibitors are well documented (5, 8, 53–62). However, systemic aldosterone or MR blockade causes hyperkalemia and acute renal insufficiency, thus requiring frequent assessment of serum electrolytes (63). Moreover, it remains elusive whether or not such blockade improves the overall mortality of patients with end-stage renal disease (2, 7, 11). Novel drugs to target the fibrotic and inflammatory injuries may be beneficial to slow the progressive loss of renal function (1, 64, 65). The present results reveal that lipocalin-2 derived from adipose tissue mediates aldosterone-induced cellular, fibrotic, and inflammatory injuries in the kidney, thus representing a potentially novel drug target for CKD and end-stage renal failure.

As a surrogate biomarker for AKI and CKD, lipocalin-2 also plays an active role in causing kidney tissue injuries (30, 65–68). Mice without lipocalin-2 are protected against nephron reduction–induced glomerulosclerosis, tubular cystic dilation, and interstitial fibrosis, as well as mononuclear cell infiltrations (43, 66). Deletion of *lcn2* alleles significantly attenuates renal injuries in mice with either genetically or chemically induced proteinuria (43). Despite this information, the precise source and the pathological form of lipocalin-2 that causes renal injuries remain unknown. After injury, lipocalin-2 protein is detected in

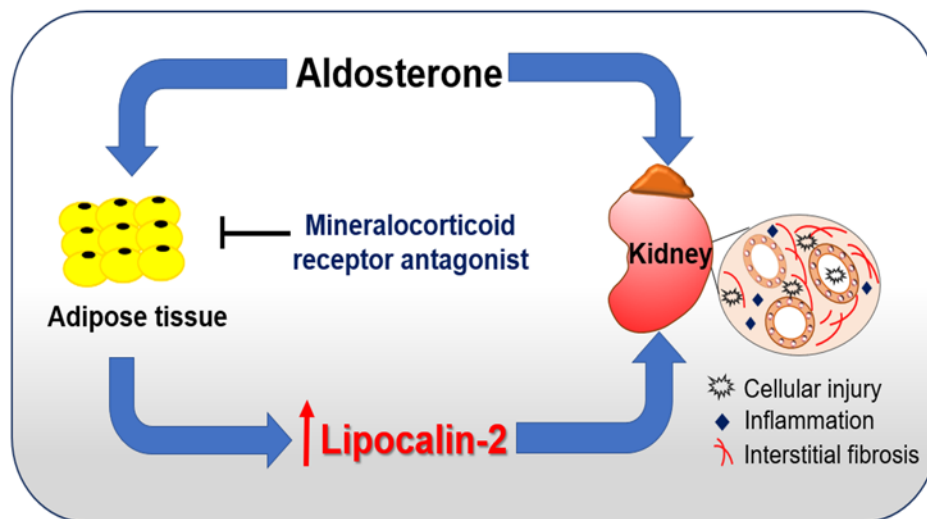


Figure 8. A working model proposing that adipose-derived lipocalin-2 mediates aldosterone-induced renal injuries. Aldosterone, a key hormonal mediator of renal disease, induces the production of lipocalin-2 from adipose tissue, which subsequently causes cellular, inflammatory, and fibrotic damages in kidney. Mineralocorticoid receptor antagonists act mainly in adipose tissue to block lipocalin-2 production, in turn alleviating aldosterone-induced renal injuries.

the damaged proximal tubules, whereas its mRNA expressions are upregulated in the loop of Henle and the collecting ducts (27, 65, 66). The present study demonstrates that, in kidney, lipocalin-2 was mainly produced by *Wt1*-expressing cells. Compared with WT animals, the expression levels of *lcn2* mRNA and lipocalin-2 protein were both decreased by more than 80% and could not be upregulated by aldosterone or ANS treatment in kidneys of *Wt1*-LKO mice. Aldosterone, ANS and exogenous lipocalin-2 (data not shown) induced acute as well as chronic injuries in kidneys of *Wt1^{Cre}GFP*-LKO mice that lack the renal expressions of *lcn2* alleles. Furthermore, chronic administration of recombinant lipocalin-2 caused renal injuries in mice lacking the endogenous expression of this molecule. Thus, locally expressed lipocalin-2 in kidney does not play a major role in causing aldosterone-induced renal injuries.

Urinary lipocalin-2 represents a collection of different pools of the protein, including that freely filtered through the glomerulus, released from injured tubules, as well as locally expressed and excreted (34). Understanding the contribution of individual pools of lipocalin-2 to renal injury is important for both risk assessment and disease management. The present results show that selective depletion of *lcn2* alleles in adipose tissue exerts similar protective effects as the global deficiency of the protein on ANS-induced cellular, inflammatory, and fibrotic injuries in the kidney, suggesting that lipocalin-2 produced from adipose tissue acts as a renal injury factor. This conclusion is supported by additional evidence: (a) adipose expressions of *lcn2* and lipocalin-2 were significantly upregulated by ANS treatment; (b) eplerenone suppressed the expressions of *lcn2* and lipocalin-2 in the adipose tissue; (c) ANS or aldosterone enhanced the renal expression of *lcn2* but could not induce kidney injuries in Adipo-LKO mice; and (d) transplantation of the fat pads from WT mice restored the ability of aldosterone to induce AKI in LKO animals. The results collectively support the conclusion that systemic sources but not the local expression/production of lipocalin-2 is responsible for chronic renal injuries. In particular, adipose tissue-derived lipocalin-2 represents a pathogenic factor escaping into the glomerular filtrate during proteinuria to promote the development of cellular and tubulointerstitial lesions.

Endogenous lipocalin-2 exists in different forms, due largely to ligand binding and posttranslational modifications (44, 45). For example, polyamination of lipocalin-2 facilitates its clearance from the circulation (44). Excessive tissue accumulation of nonpolyaminated lipocalin-2 causes vascular and cardiac dysfunctions (23, 44). Certain forms of lipocalin-2 are filtered by the kidney but bypass sites of megalin-dependent recapture (69). Other forms are less efficiently excreted in the urine under physiological conditions (23). The present study revealed that aldosterone facilitated the urinary excretion of lipocalin-2, in particular that of R81E, which induced AKI and CKD independent of the local *lcn2* expressions in the kidney. Moreover, the R81E form of lipocalin-2 was present in the circulation and urine samples of human subjects. The amount of urinary R81E was independently correlated with kidney injury markers,

suggesting that this form of lipocalin-2 represents a better biomarker for AKI and CKD than other forms (70). Lipocalin-2 binds to ferric enterobactin by interacting with 3 positively charged residues (R81, K125, and K134), whereby the complex lipocalin-2/catechols/iron (III) is formed and ready for excretion. Such binding with the residues K125 and K134 is pH dependent, as the binding of the catechols to lipocalin-2 is reduced in acidic environment (71). This may provide an explanation for the observation that R81E is the most excreted form of lipocalin-2 because of its pH-independent properties. After fat pad transplantation from WT to LKO mice, aldosterone increased a significant amount of lipocalin-2 in the urine but not serum, suggesting that certain properties of lipocalin-2 derived from adipose tissue allow this protein to be filtered more efficiently and causes injuries in kidney. A broad range of nonpolar ligands binds to the lipophilic site of lipocalin-2 and changes the conformation of the molecule (72). Depending on the origin, the complex of lipocalin-2 and its tissue-specific ligands may exert different functions. In addition, the folding of lipocalin-2, especially of its lipophilic binding pocket, is sensitive to the change of environmental polarity (73). For example, the composition of urine controls the biological activity of excreted lipocalin-2 (74). Thus, understanding how lipocalin-2 derived from adipose tissue differs from other sources of this molecule should provide important insights on its pathological role in kidney injury.

Multiple pathways may contribute to adipose lipocalin-2-mediated renal injury. First, endocytosis of adipose-derived lipocalin-2 by proximal tubules leads to acute cell loss by apoptosis and the subsequent proliferative and inflammatory kidney damages (27, 66, 75). During development, lipocalin-2 is expressed in the early epithelial progenitors to trigger the epithelialization of kidney mesenchyme and the formation of nephrons (76–78). After injury, local expression of lipocalin-2 is tightly correlated with cell proliferation and mediates the mitogenic effect of growth factors in the kidney (66). Exogenous lipocalin-2 can induce endogenous *lcn2* expression in the kidney (data not shown). Locally synthesized lipocalin-2 is unlikely to be introduced back into the circulation but rather is excreted into the urine (79). At this stage, it is not known whether the increased local *lcn2* expression occurred only in Wt1 cells or also in other renal cell types, such as the inner medulla collecting duct (mIMCD-3) cells. In the latter, lipocalin-2 induces apoptosis by promoting the generation of ROS (43). Second, the presence of adipose tissue-derived lipocalin-2 may stimulate the local expression of *lcn2* that further amplifies aldosterone/MR signaling in kidney. Without lipocalin-2, the *nr3c2* expression was significantly lower in kidney and adipose tissues of LKO than those of WT mice and could not be upregulated by ANS or aldosterone. Acute treatment with lipocalin-2 protein plus aldosterone increased *nr3c2* in WT but not LKO kidneys (data not shown). Chronic treatment with R81E significantly increased the renal expression of *hsd3b1* and the excretion of urinary aldosterone. Thus, a reinforcing loop may exist between local *lcn2* and *nr3c2* expressions in the kidney that facilitates the nonrenal source of lipocalin-2 to induce AKI, CKD, and end-stage renal failure (Figure 8). In addition, it is tempting to hypothesize that *lcn2* expressed in Wt1-positive cells controls cell proliferation and apoptosis in response to kidney damage, which may explain that constitutive deletion of *lcn2* alleles largely prevented the glomerulopathy in ANS-treated LKO mice, whereas Adipo-LKO mice exhibited less protection in regard to the enlargement of kidney and glomeruli, as well as in regard to the downregulation of synaptopodin. During embryonic development, Wt1 is transiently expressed in the early proepicardium and epicardium but is continuously required for nephrogenesis, especially the formation of mature glomeruli (80). In adult animals, Wt1 is only expressed in rare cell populations but acts as a major regulator of the homeostasis of some organs, such as kidney (81). Thus, aldosterone and/or lipocalin-2 may regulate *lcn2* expression in Wt1-positive cells to cause glomerular injuries.

In summary, the present study provides evidence that lipocalin-2 derived from adipose tissue contributes to the development of CKD by enhancing cellular, inflammatory, and fibrotic injuries. This conclusion is in line with the observations in patients that long-term increases in urinary lipocalin-2 levels accelerate renal fibrosis (82, 83). Collectively, the present information supports the concept that lipocalin-2 derived from adipose tissues is the key pathological link between proteinuria and the development of tubulointerstitial lesions and suggests that targeting the urinary excretion of pathological forms of lipocalin-2 may help to prevent the development of end-stage renal failure.

Methods

Animal models. The breeders of various mouse models were housed in a specific pathogen free temperature- and humidity-controlled room (25°C ± 1°C and 50%–70%, respectively), under a 12-hour dark/12-hour light cycle and with free access to water and food. Mice without lipocalin-2 expression (LKO) or with

the *lcn2* alleles flanked by LoxP (*Lcn2*-floxed) were maintained on a C57BL/6J background (23, 44, 84). Mice harboring Adipoq-Cre BAC transgene (stock no. 010803), *Wt1*^{CreGFP} (stock no. 010911), or *Wt1*^{CreERT2} knock-in allele (stock no. 010912) were obtained from the Jackson Laboratory and subsequently cross-bred with the *Lcn2*-floxed mice to produce litters lacking lipocalin-2 expression specifically in adipose tissue (Adipo-LKO) and *Wt1*-expressing cells (*Wt1*^{CreGFP}-LKO or *Wt1*^{CreERT2}-LKO, collectively referred to as *Wt1*-LKO), respectively. The *Wt1*-LKO mice were maintained as the heterozygotes for the *Wt1*^{CreGFP} and *Wt1*^{CreERT2} knock-in alleles, thus avoiding the developmental defects of the epicardium (85). Prior to the experiment, *Wt1*^{CreERT2}-LKO mice were i.p. injected with 33 mg/kg/day of tamoxifen (MilliporeSigma) for 5 consecutive days to induce the Cre-recombination (86). The primers for genotyping are listed in Supplemental Table 1. Under standard housing conditions, the body weight, food intake, general appearance, and physical and social activities were not significantly different between age-matched WT, LKO, *Lcn2*-floxed, Adipo-LKO, and *Wt1*-LKO mice. For all studies, inbred C57BL/6J littermates were included as WT control animals for LKO, whereas the *Lcn2*-floxed littermates served as controls in experiments on Adipo-LKO or *Wt1*-LKO. When subjected to experimental conditions, the *Lcn2*-floxed littermates exhibited a similar extent of renal damages and changes in arterial blood pressure as those of WT control animals. Thus, the results for *Lcn2*-floxed littermates were not included for presentation.

Surgical procedure and drug treatment. Male mice (12 weeks old) were anesthetized by i.p. injection with a diluted mixture of Hypnorm (0.315 mg/ml of fentanyl and 10 mg/ml of fluanisone; VetaPharma Ltd.) and Dormicum (5 mg/ml of midazolam; Roche Diagnostics) in water (Hypnorm/Dormicum/water = 1:1:6) at a dose of 10 μ l/g. After left uninephrectomy, ALZET osmotic minipumps (Durect Corporation) filled with aldosterone (200 μ g/kg/day; MilliporeSigma) were implanted s.c. For postoperative care, meloxicam (5 mg/kg; Boehringer Ingelheim) was added into the drinking water for 3 days after surgery. The drinking water was subsequently replaced with 1% sodium chloride (MilliporeSigma) in water. The kidney of the sham control mice was exposed but not removed. During the following 4 weeks, both aldosterone/uninephrectomy/salt-treated (ANS-treated) and sham-treated mice were fed with standard chow. Eplerenone (100 mg/kg/day; Selleckchem) or vehicle were given to the ANS-treated mice in the drinking water (according to their daily consumption of 30 ± 6 ml) from the second week after surgery until the end of the experiment. Body weight, food and water intake, fat mass composition, and serum lipocalin-2 levels were monitored weekly. Animals were put in metabolic cages fortnightly (Tecniplast Gazzada, 3701MO-000). The 24-hour urine was collected from individual mice with free access to food and water. Systolic and diastolic arterial blood pressures were measured by tail cuff plethysmography (Visitech Systems) (87). Fat transplantation was performed in anesthetized animals as described (88). Briefly, the s.c. (~0.3 g) and epididymal (~0.7 g) fat pads were collected from 10-week-old WT animals and transplanted into the dorsal s.c. and left inguinal area of age- and sex-matched LKO mice.

For acute treatment, mice were administered with either saline or aldosterone (2 mg/kg; s.c.) prior to injection of human lipocalin-2 recombinant proteins (10 μ g/mouse; i.p.). They were then placed in the metabolic cages to collect the 24-hour urine. At the end of treatment, the mice were sacrificed for serum and tissue collections. Chronic treatment was performed by daily injection (i.p.) with vehicle or human lipocalin-2 recombinant proteins (10 μ g/mouse) for 4 weeks. At the end of treatment, the mice were euthanized with 100 μ l of a 10:1 mixture of ketamine (100 mg/ml) and xylazine (100 mg/ml; both from MilliporeSigma) prior to organ/tissue collections. Loss of consciousness and suppression of reflexes (absence of withdrawal reflex, tail-pinch response, and limb muscle tone with regular heart and respiratory rates) were checked to ensure sufficient anesthesia.

Endogenous murine or exogenous human lipocalin-2 were measured using specific ELISA kits (Immunodiagnosics, Hong Kong, China). Briefly, 30 μ g of kidney and 50 μ g of adipose tissue lysates were prepared in lysis buffer containing 10 mM Tris (pH 7.4), 140 mM NaCl, 1 mM EDTA, 1% Triton X-100, and 1 mM PMSF to examine the levels of lipocalin-2. Serum was diluted 1 in 80 and urine was diluted 1 in 20, respectively, for the ELISA. The urine samples were diluted 1 in 5 or 1 in 10 to examine the levels of renal injury markers, including kidney injury molecule-1 (Kim-1; R&D Systems) (42), albumin (Exocell Inc.), and aldosterone (Arbor Assays). All chemicals obtained from MilliporeSigma, unless otherwise indicated.

Expression and purification of recombinant lipocalin-2. The prokaryotic plasmids including pPRO-His-hLCN2, pPRO-His-hLCN2-C87A, pPRO-His-hLCN2-R81E, pPRO-His-hLCN2-K134E, and pPRO-His-hLCN2-K125E were constructed and transformed into BL21 CodonPlus(DE3)-RIL Competent cells (Agilent Technologies) to express hLcn2, and the mutants of lipocalin-2 with cysteine C87A, R81E, K125E, or

K134E (22, 44). All the recombinant proteins contained an NH₂-terminal polyhistidine tag for affinity purification using Ni-NTA Agarose (QIAGEN). Endotoxin was removed by a Detoxi-gel Endotoxin-Removal Gel (Pierce Biotechnology Inc.), and the purity of individual lipocalin-2 variants was confirmed by SDS-PAGE and fast protein liquid chromatography analysis.

Histological staining. Kidney and adipose tissues were fixed in 10% neutral-buffered formaldehyde for 24 hours and then transferred to 70% ethanol for storage at 4°C. The fixed tissues were dehydrated in a Leica ASP200 S Tissue Processor (Leica Biosystems) and embedded in paraffin until further use. Tissue sections (2.5 μm) were prepared with a HM 340E Electronic Rotary Microtome (Thermo Fisher Scientific) and dried overnight at 40°C. Tissue sections were subsequently deparaffinized, rehydrated, and stained with H&E as described (23). For PAS staining, tissue sections prepared as above were placed in 1% periodic acid solution (MilliporeSigma) for 5 minutes. After rinsing with distilled water, Schiff's reagent (MilliporeSigma) was applied for 15 minutes at room temperature, followed by hematoxylin counterstaining for 30 seconds. PSR staining was performed using 0.1% Sirius red in saturated aqueous picric acid (MilliporeSigma). The sections were dehydrated in ethanol, cleared with xylene, and mounted in Histofluid mounting medium (Mariesfeld-Superior) for subsequent imaging analyses.

IHC. Kidney and adipose tissue sections, prepared as above, were placed in 3% hydrogen peroxide for 30 minutes before adding boiling sodium citrate buffer (10 mM, pH 6.0) for 10 minutes. After antigen retrieval, the slides were blocked with 5% BSA and then incubated with antibodies against murine lipocalin-2 (Immunodiagnosics; catalog 12050) or macrophage marker F4/80 (clone CI:A3-1, Thermo Fisher Scientific) overnight at 4°C. Streptavidin horseradish peroxidase-conjugated secondary antibodies were applied to the tissue sections for 1 hour at room temperature. After washing 3 times, the slides were developed with 3,3'-diaminobenzidine (DAB; MilliporeSigma) and counterstained in hematoxylin solution. All images were visualized and captured with an Olympus BX41 microscope and a DP72 camera.

Histological assessment of renal damages. To qualify glomerular injury, images with a magnification of 400× were used. At least 30 PAS-stained glomerular hilar cross-sections were analyzed from each kidney sample to determine glomerular area and volume using the ImageJ software (version 1.50, NIH) (89). Briefly, after identifying glomeruli with both arterioles and proximal tubule in the same cross section, the outline of the glomerular area was manually traced for the measurement. The glomerular volume V_G was calculated as $V_G = (\beta/k)(A_m)^{3/2}$, where $\beta = 1.38$ (shape coefficient for spheres), $k = 1.1$ (size distribution coefficient), and A_m is the surface area. Tubular hypertrophy was evaluated by measuring the diameter and height of at least 30 proximal tubules in each section at 400× magnification. The line morphometric tool of ImageJ was used to measure the inner lumen and the height of renal epithelial cells inside the proximal tubules (89). Interstitial volume was also measured using ImageJ. First, the images were converted to greyscale in order to set up the threshold levels for the staining detection. Then, once the threshold was applied, images were converted to binary (black and white) followed by region of interest (ROI) measurement using the freehand tool. To determine area stained within the ROI, selecting Analyze/Analyze Particles revealed a summary that included the area fraction for the proportion of the ROI with positive staining (89).

In situ hybridization. Eleven pairs of double Z oligo probes (RNAscope Probe-Mm-Lcn2; catalog 313971), each containing 18-25 bp, were designed to target the 1–640 bp of murine *Lcn2* (NCBI NM_008491.1) and synthesized by Advanced Cell Diagnostics. In situ hybridization was performed using the RNAscope Intro Pack 2.5 HD Reagent Kit BROWN – Mm (catalog 322371, Advanced Cell Diagnostics). Briefly, freshly prepared kidney tissue sections (5 μm) were exposed to RNAscope hydrogen peroxide for 10 minutes at room temperature, followed by RNAscope Target Retrieval Reagent (Advanced Cell Diagnostics) during 40 minutes at 99°C. RNAscope Protease Plus was then applied to the tissue sections for 30 minutes before incubating them with the RNA probe for another 2 hours at 40°C. After 6 steps of amplification, the hybridization signals were developed by applying the RNAscope DAB reagent. All sections were counterstained with hematoxylin before mounting on glass coverslips with a xylene based mounting medium.

Western blotting. A precooled TissueLyserLT (QIAGEN) was used to homogenize tissue samples in a buffer containing 20 mM Tris-HCl (pH 7.5), 1% Triton X-100, 150 mM NaCl, 1 mM Na₂EDTA, 1 mM EGTA, 1% sodium deoxycholate, 2.5 mM sodium pyrophosphate, 1 mM sodium fluoride, 1 mM sodium orthovanadate, and protease inhibitor cocktails (Roche Diagnostics). The protein concentrations of the tissue lysates were determined using the Bicinchoninic Acid Assay (Pierce Biotechnology Inc.). Serum samples (1.5 μl) or tissue lysates (50 or 150 μg) were incubated with a Laemmli sample buffer, boiled for 10 minutes, and separated by SDS-PAGE. After transferring to 0.2 μm FluoroTrans W PVDF transfer

membranes (Pall Corporation) and blocking with 5% BSA, antibodies against synaptopodin (clone N-14; Santa Cruz Biotechnology Inc.) were applied for overnight incubation at 4°C. The immuno-complexes recognized by the secondary antibodies were detected with enhanced chemiluminescence reagents (GE Healthcare). β -Actin was probed as a loading control for normalization and quantitative comparisons.

Quantitative PCR. Total RNA was extracted from kidney and adipose tissues for reverse transcription and quantitative PCR (qPCR) analysis as described (44). Briefly, 500 ng total RNA were prepared for reverse transcription using a PrimeScript RT reagent Kit (Takara Bio Inc.), followed by qPCR using a QuantiTect SYBR Green PCR Kit (QIAGEN). All reactions were performed in an ABI PRISM 7900 HT Sequence Detection System (Applied Biosystems). The primer sequences for qPCR are listed in Supplemental Table 2. After normalization against β -actin, the differences between the Δ Ct values were calculated to obtain fold changes for comparison between different groups.

ELISA for human samples. The demographic and clinical characteristics of the healthy volunteer cohort including 100 human subjects has been reported (23). Polyclonal antibodies against hLcn2, C87A, and R81E were produced in New Zealand female rabbits and used to establish the specific sandwich ELISA kits as described (22, 23, 44). Briefly, to compare the presence of hLcn2, C87A, and R81E proteins in samples from human healthy volunteers, plasma and urine were both diluted at 1:25 for a 1-hour incubation at 37°C in the coated ELISA plates. After washing, biotinylated antibodies were applied for another hour. The immunocomplexes were detected with streptavidin-conjugated horseradish peroxidase and substrates. The reactions were stopped prior to the measurement of absorbance at 450 nm with a plate reader (Biotek Instruments Inc.). Kim-1 (R&D Systems), haptoglobin (Biovender), aldosterone (Cayman Chemical) and albumin (Exocell Inc.) were examined in urine samples using their specific ELISA kits. Serum cystatin C was measured using a clinical chemistry analyzer as per manufacturer's protocol (Olympus AU400). The amount of creatinine was assayed in both plasma and urine samples according to the manufacturer's instructions (Abcam). The urine ACR was calculated to evaluate the renal function, with ACR <3 mg/mmol considered to be normal, 3–30 mg/mmol to be moderately increased, and >30 mg/mmol to be severely augmented (90).

Statistics. All experiments were repeated at least 3 times using different sets of experimental animals. All analyses were performed using Prism version 7.0 (GraphPad Software Inc.). One-way ANOVA with the Bonferroni post hoc test was used for statistical comparisons of repeated measures and multiple groups of data. Mann-Whitney *U* tests and 2-tailed Student's *t* test were used for statistical comparisons between 2 groups of continuous variables (including QPCR, ELISA, and image quantifications). Values are presented as mean \pm SEM. For all statistical comparisons, *P* values less than 0.05 were accepted to indicate significant differences.

For human studies, statistical calculations were performed using the IBM SPSS version 21.0 software. Data are expressed as medians with interquartile range. Partial Pearson correlations were used to examine the relationship between variables of interest, with adjustment for age, smoking, and BMI. *P* values less than 0.05 indicated a significant difference in all statistical comparisons.

Study approval. All experimental procedures were approved by the Committee on the Use of Live Animals for Teaching and Research of the University of Hong Kong and performed in accordance with the *Guide for the Care and Use of Laboratory Animals* (National Academies Press, 2011). The human study was approved by the IRB of the University of Hong Kong/Hospital Authority Hong Kong West Cluster (reference number UW 14-044).

Author contributions

WYS, BB, CL, KY, and DL performed the experiment and acquired the data; WYS, BB, KY, and YW conducted the data analyses, results organization, and interpretation; MF, NV, AX, PMV, and YW designed the research; DW, YZ, JY, AX, and YW provided the reagents; WYS, BB, PMV, and YW wrote the manuscript.

Acknowledgments

This work was financially supported by the grants from Research Grant Council of Hong Kong (General Research Fund 17121714 and 17117017), Collaborative Research Fund of Hong Kong (C7055-14G), Les Laboratoires Servier (RS140130), an international collaborative fund by the Guangzhou Municipal Bureau of Science and Technology (2016201604030030), and the State Key Laboratory of Pharmaceutical Biotechnology.

Address correspondence to: Yu Wang, Level 2, Laboratory Block, 21 Sassoon Road, Pokfulam, Hong Kong. Phone: 852.39176864; Email: yuwanghk@hku.hk.

1. Stefoni S, Cianciolo G, Baraldi O, Iorio M, Angelini ML. Emerging drugs for chronic kidney disease. *Expert Opin Emerg Drugs*. 2014;19(2):183–199.
2. Remuzzi G, Perico N, Macia M, Ruggenenti P. The role of renin-angiotensin-aldosterone system in the progression of chronic kidney disease. *Kidney Int Suppl*. 2005;(99):S57–S65.
3. Wolf G, Ritz E. Combination therapy with ACE inhibitors and angiotensin II receptor blockers to halt progression of chronic renal disease: pathophysiology and indications. *Kidney Int*. 2005;67(3):799–812.
4. Bomback AS, Rektman Y, Klemmer PJ, Canetta PA, Radhakrishnan J, Appel GB. Aldosterone breakthrough during aliskiren, valsartan, and combination (aliskiren + valsartan) therapy. *J Am Soc Hypertens*. 2012;6(5):338–345.
5. Chrysostomou A, Becker G. Spironolactone in addition to ACE inhibition to reduce proteinuria in patients with chronic renal disease. *N Engl J Med*. 2001;345(12):925–926.
6. Terata S, et al. Plasma renin activity and the aldosterone-to-renin ratio are associated with the development of chronic kidney disease: the Ohasama Study. *J Hypertens*. 2012;30(8):1632–1638.
7. Schwenk MH, Hirsch JS, Bomback AS. Aldosterone blockade in CKD: emphasis on pharmacology. *Adv Chronic Kidney Dis*. 2015;22(2):123–132.
8. Sato A. The necessity and effectiveness of mineralocorticoid receptor antagonist in the treatment of diabetic nephropathy. *Hypertens Res*. 2015;38(6):367–374.
9. Vardeny O, et al. Influence of baseline and worsening renal function on efficacy of spironolactone in patients With severe heart failure: insights from RALES (Randomized Aldactone Evaluation Study). *J Am Coll Cardiol*. 2012;60(20):2082–2089.
10. Cooper LB, et al. Use of Mineralocorticoid Receptor Antagonists in Patients With Heart Failure and Comorbid Diabetes Mellitus or Chronic Kidney Disease. *J Am Heart Assoc*. 2017;6(12).
11. Schrier RW, Masoumi A, Elhassan E. Aldosterone: role in edematous disorders, hypertension, chronic renal failure, and metabolic syndrome. *Clin J Am Soc Nephrol*. 2010;5(6):1132–1140.
12. Guo C, et al. Mineralocorticoid receptor blockade reverses obesity-related changes in expression of adiponectin, peroxisome proliferator-activated receptor-gamma, and proinflammatory adipokines. *Circulation*. 2008;117(17):2253–2261.
13. Penforis P, Viengchareun S, Le Menuet D, Cluzeaud F, Zennaro MC, Lombès M. The mineralocorticoid receptor mediates aldosterone-induced differentiation of T37i cells into brown adipocytes. *Am J Physiol Endocrinol Metab*. 2000;279(2):E386–E394.
14. Rondinone CM, Rodbard D, Baker ME. Aldosterone stimulated differentiation of mouse 3T3-L1 cells into adipocytes. *Endocrinology*. 1993;132(6):2421–2426.
15. Valero-Muñoz M, et al. Heart Failure With Preserved Ejection Fraction Induces Beiging in Adipose Tissue. *Circ Heart Fail*. 2016;9(1):e002724.
16. Kraus D, Jäger J, Meier B, Fasshauer M, Klein J. Aldosterone inhibits uncoupling protein-1, induces insulin resistance, and stimulates proinflammatory adipokines in adipocytes. *Horm Metab Res*. 2005;37(7):455–459.
17. Sechi LA, Colussi G, Di Fabio A, Catena C. Cardiovascular and renal damage in primary aldosteronism: outcomes after treatment. *Am J Hypertens*. 2010;23(12):1253–1260.
18. Nguyen Dinh Cat A, et al. Adipocyte-Specific Mineralocorticoid Receptor Overexpression in Mice Is Associated With Metabolic Syndrome and Vascular Dysfunction: Role of Redox-Sensitive PKG-1 and Rho Kinase. *Diabetes*. 2016;65(8):2392–2403.
19. Urbanet R, et al. Adipocyte Mineralocorticoid Receptor Activation Leads to Metabolic Syndrome and Induction of Prostaglandin D2 Synthase. *Hypertension*. 2015;66(1):149–157.
20. Hirata A, et al. Blockade of mineralocorticoid receptor reverses adipocyte dysfunction and insulin resistance in obese mice. *Cardiovasc Res*. 2009;84(1):164–172.
21. Luo P, et al. Aldosterone deficiency prevents high-fat-feeding-induced hyperglycaemia and adipocyte dysfunction in mice. *Diabetologia*. 2013;56(4):901–910.
22. Wang Y, et al. Lipocalin-2 is an inflammatory marker closely associated with obesity, insulin resistance, and hyperglycemia in humans. *Clin Chem*. 2007;53(1):34–41.
23. Yang K, et al. Measuring non-polyaminated lipocalin-2 for cardiometabolic risk assessment. *ESC Heart Fail*. 2017;4(4):563–575.
24. Wang Y. Small lipid-binding proteins in regulating endothelial and vascular functions: focusing on adipocyte fatty acid binding protein and lipocalin-2. *Br J Pharmacol*. 2012;165(3):603–621.
25. Kjeldsen L, Johnsen AH, Sengeløv H, Borregaard N. Isolation and primary structure of NGAL, a novel protein associated with human neutrophil gelatinase. *J Biol Chem*. 1993;268(14):10425–10432.
26. Cowland JB, Borregaard N. Molecular characterization and pattern of tissue expression of the gene for neutrophil gelatinase-associated lipocalin from humans. *Genomics*. 1997;45(1):17–23.
27. Schmidt-Ott KM, et al. Dual action of neutrophil gelatinase-associated lipocalin. *J Am Soc Nephrol*. 2007;18(2):407–413.
28. Mishra J, et al. Neutrophil gelatinase-associated lipocalin (NGAL) as a biomarker for acute renal injury after cardiac surgery. *Lancet*. 2005;365(9466):1231–1238.
29. Elmedany SM, Naga SS, Elsharkawy R, Mahrous RS, Elnaggar AI. Novel urinary biomarkers and the early detection of acute kidney injury after open cardiac surgeries. *J Crit Care*. 2017;40:171–177.
30. Bolignano D, et al. Neutrophil gelatinase-associated lipocalin (NGAL) and progression of chronic kidney disease. *Clin J Am Soc Nephrol*. 2009;4(2):337–344.
31. Bolignano D, Coppolino G, Lacquaniti A, Nicocia G, Buemi M. Pathological and prognostic value of urinary neutrophil gelatinase-associated lipocalin in macroproteinuric patients with worsening renal function. *Kidney Blood Press Res*. 2008;31(4):274–279.
32. Bolignano D, et al. Urinary neutrophil gelatinase-associated lipocalin (NGAL) is associated with severity of renal disease in proteinuric patients. *Nephrol Dial Transplant*. 2008;23(1):414–416.
33. Donadio C. Effect of glomerular filtration rate impairment on diagnostic performance of neutrophil gelatinase-associated lipo-

- calin and B-type natriuretic peptide as markers of acute cardiac and renal failure in chronic kidney disease patients. *Crit Care*. 2014;18(1):R39.
34. Kuwabara T, et al. Urinary neutrophil gelatinase-associated lipocalin levels reflect damage to glomeruli, proximal tubules, and distal nephrons. *Kidney Int*. 2009;75(3):285–294.
35. Tarjus A, et al. Neutrophil Gelatinase-Associated Lipocalin, a Novel Mineralocorticoid Biotarget, Mediates Vascular Profibrotic Effects of Mineralocorticoids. *Hypertension*. 2015;66(1):158–166.
36. Leopold JA. The Central Role of Neutrophil Gelatinase-Associated Lipocalin in Cardiovascular Fibrosis. *Hypertension*. 2015;66(1):20–22.
37. Hall ME, do Carmo JM, da Silva AA, Juncos LA, Wang Z, Hall JE. Obesity, hypertension, and chronic kidney disease. *Int J Nephrol Renovasc Dis*. 2014;7:75–88.
38. Sarzani R, Guerra F, Mancinelli L, Buglioni A, Franchi E, Dessi-Fulgheri P. Plasma aldosterone is increased in class 2 and 3 obese essential hypertensive patients despite drug treatment. *Am J Hypertens*. 2012;25(7):818–826.
39. Vecchiola A, Lagos CF, Carvajal CA, Baudrand R, Fardella CE. Aldosterone Production and Signaling Dysregulation in Obesity. *Curr Hypertens Rep*. 2016;18(3):20.
40. Srichai MB, et al. A WT1 co-regulator controls podocyte phenotype by shuttling between adhesion structures and nucleus. *J Biol Chem*. 2004;279(14):14398–14408.
41. Yanagida-Asanuma E, et al. Synaptopodin protects against proteinuria by disrupting Cdc42:IRSp53:Mena signaling complexes in kidney podocytes. *Am J Pathol*. 2007;171(2):415–427.
42. Wasung ME, Chawla LS, Madero M. Biomarkers of renal function, which and when? *Clin Chim Acta*. 2015;438:350–357.
43. El Karoui K, et al. Endoplasmic reticulum stress drives proteinuria-induced kidney lesions via Lipocalin 2. *Nat Commun*. 2016;7:10330.
44. Song E, et al. Deamidated lipocalin-2 induces endothelial dysfunction and hypertension in dietary obese mice. *J Am Heart Assoc*. 2014;3(2):e000837.
45. Kjeldsen L, Cowland JB, Borregaard N. Human neutrophil gelatinase-associated lipocalin and homologous proteins in rat and mouse. *Biochim Biophys Acta*. 2000;1482(1-2):272–283.
46. Sia AK, Allred BE, Raymond KN. Siderocalins: Siderophore binding proteins evolved for primary pathogen host defense. *Curr Opin Chem Biol*. 2013;17(2):150–157.
47. Goetz DH, Holmes MA, Borregaard N, Bluhm ME, Raymond KN, Strong RK. The neutrophil lipocalin NGAL is a bacteriostatic agent that interferes with siderophore-mediated iron acquisition. *Mol Cell*. 2002;10(5):1033–1043.
48. Hostetter TH, Rosenberg ME, Ibrahim HN, Juknevicus I. Aldosterone in progressive renal disease. *Semin Nephrol*. 2001;21(6):573–579.
49. Deo R, et al. Serum aldosterone and death, end-stage renal disease, and cardiovascular events in blacks and whites: findings from the Chronic Renal Insufficiency Cohort (CRIC) Study. *Hypertension*. 2014;64(1):103–110.
50. Rocha R, Chander PN, Zuckerman A, Stier CT. Role of aldosterone in renal vascular injury in stroke-prone hypertensive rats. *Hypertension*. 1999;33(1 Pt 2):232–237.
51. Nagase M, Matsui H, Shibata S, Gotoda T, Fujita T. Salt-induced nephropathy in obese spontaneously hypertensive rats via paradoxical activation of the mineralocorticoid receptor: role of oxidative stress. *Hypertension*. 2007;50(5):877–883.
52. Blasi ER, Rocha R, Rudolph AE, Blomme EA, Polly ML, McMahon EG. Aldosterone/salt induces renal inflammation and fibrosis in hypertensive rats. *Kidney Int*. 2003;63(5):1791–1800.
53. Struthers AD, MacDonald TM. Review of aldosterone- and angiotensin II-induced target organ damage and prevention. *Cardiovasc Res*. 2004;61(4):663–670.
54. Epstein M. Aldosterone as a mediator of progressive renal disease: pathogenetic and clinical implications. *Am J Kidney Dis*. 2001;37(4):677–688.
55. Bianchi S, Bigazzi R, Campese VM. Antagonists of aldosterone and proteinuria in patients with CKD: an uncontrolled pilot study. *Am J Kidney Dis*. 2005;46(1):45–51.
56. Remuzzi G, Cattaneo D, Perico N. The aggravating mechanisms of aldosterone on kidney fibrosis. *J Am Soc Nephrol*. 2008;19(8):1459–1462.
57. Toto RD. Aldosterone blockade in chronic kidney disease: can it improve outcome? *Curr Opin Nephrol Hypertens*. 2010;19(5):444–449.
58. Waanders F, et al. Aldosterone, from (patho)physiology to treatment in cardiovascular and renal damage. *Curr Vasc Pharmacol*. 2011;9(5):594–605.
59. Bianchi S, Bigazzi R, Campese VM. Long-term effects of spironolactone on proteinuria and kidney function in patients with chronic kidney disease. *Kidney Int*. 2006;70(12):2116–2123.
60. Chrysostomou A, Pedagogos E, MacGregor L, Becker GJ. Double-blind, placebo-controlled study on the effect of the aldosterone receptor antagonist spironolactone in patients who have persistent proteinuria and are on long-term angiotensin-converting enzyme inhibitor therapy, with or without an angiotensin II receptor blocker. *Clin J Am Soc Nephrol*. 2006;1(2):256–262.
61. van den Meiracker AH, et al. Spironolactone in type 2 diabetic nephropathy: Effects on proteinuria, blood pressure and renal function. *J Hypertens*. 2006;24(11):2285–2292.
62. Epstein M, et al. Selective aldosterone blockade with eplerenone reduces albuminuria in patients with type 2 diabetes. *Clin J Am Soc Nephrol*. 2006;1(5):940–951.
63. Cooper LB, et al. Use of Mineralocorticoid Receptor Antagonists in Patients With Heart Failure and Comorbid Diabetes Mellitus or Chronic Kidney Disease. *J Am Heart Assoc*. 2017;6(12):e006540.
64. Shavit L, Lifschitz MD, Epstein M. Aldosterone blockade and the mineralocorticoid receptor in the management of chronic kidney disease: current concepts and emerging treatment paradigms. *Kidney Int*. 2012;81(10):955–968.
65. Mori K, Nakao K. Neutrophil gelatinase-associated lipocalin as the real-time indicator of active kidney damage. *Kidney Int*. 2007;71(10):967–970.
66. Viau A, et al. Lipocalin 2 is essential for chronic kidney disease progression in mice and humans. *J Clin Invest*. 2010;120(11):4065–4076.

67. Ding H, et al. Urinary neutrophil gelatinase-associated lipocalin (NGAL) is an early biomarker for renal tubulointerstitial injury in IgA nephropathy. *Clin Immunol.* 2007;123(2):227–234.
68. Wei F, et al. Neutrophil gelatinase-associated lipocalin suppresses cyst growth by Pkd1 null cells in vitro and in vivo. *Kidney Int.* 2008;74(10):1310–1318.
69. Barasch J, et al. Disposal of iron by a mutant form of lipocalin 2. *Nat Commun.* 2016;7:12973.
70. Krstic D, et al. Biochemical Markers of Renal Function. *Curr Med Chem.* 2016;23(19):2018–2040.
71. Bao GH, Ho CT, Barasch J. The Ligands of Neutrophil Gelatinase-Associated Lipocalin. *RSC Adv.* 2015;5(126):104363–104374.
72. Chu ST, Lin HJ, Huang HL, Chen YH. The hydrophobic pocket of 24p3 protein from mouse uterine luminal fluid: fatty acid and retinol binding activity and predicted structural similarity to lipocalins. *J Pept Res.* 1998;52(5):390–397.
73. Glasgow BJ, et al. A conserved disulfide motif in human tear lipocalins influences ligand binding. *Biochemistry.* 1998;37(8):2215–2225.
74. Shields-Cutler RR, et al. Human Urinary Composition Controls Antibacterial Activity of Siderocalin. *J Biol Chem.* 2015;290(26):15949–15960.
75. Langelueddecke C, Roussa E, Fenton RA, Wolff NA, Lee WK, Thévenod F. Lipocalin-2 (24p3/neutrophil gelatinase-associated lipocalin (NGAL)) receptor is expressed in distal nephron and mediates protein endocytosis. *J Biol Chem.* 2012;287(1):159–169.
76. Barasch J, et al. Mesenchymal to epithelial conversion in rat metanephros is induced by LIF. *Cell.* 1999;99(4):377–386.
77. Barasch J, Pressler L, Connor J, Malik A. A ureteric bud cell line induces nephrogenesis in two steps by two distinct signals. *Am J Physiol.* 1996;271(1 Pt 2):F50–F61.
78. Yang J, et al. An iron delivery pathway mediated by a lipocalin. *Mol Cell.* 2002;10(5):1045–1056.
79. Shrestha K, Shao Z, Singh D, Dupont M, Tang WH. Relation of systemic and urinary neutrophil gelatinase-associated lipocalin levels to different aspects of impaired renal function in patients with acute decompensated heart failure. *Am J Cardiol.* 2012;110(9):1329–1335.
80. Moore AW, McInnes L, Kreidberg J, Hastie ND, Schedl A. YAC complementation shows a requirement for Wt1 in the development of epicardium, adrenal gland and throughout nephrogenesis. *Development.* 1999;126(9):1845–1857.
81. Chau YY, et al. Acute multiple organ failure in adult mice deleted for the developmental regulator Wt1. *PLoS Genet.* 2011;7(12):e1002404.
82. Entin-Meer M, et al. Accelerated renal fibrosis in cardiorenal syndrome is associated with long-term increase in urine neutrophil gelatinase-associated lipocalin levels. *Am J Nephrol.* 2012;36(2):190–200.
83. Nakagawa S, et al. Molecular Markers of Tubulointerstitial Fibrosis and Tubular Cell Damage in Patients with Chronic Kidney Disease. *PLoS One.* 2015;10(8):e0136994.
84. Law IK, et al. Lipocalin-2 deficiency attenuates insulin resistance associated with aging and obesity. *Diabetes.* 2010;59(4):872–882.
85. Zhou B, et al. Epicardial progenitors contribute to the cardiomyocyte lineage in the developing heart. *Nature.* 2008;454(7200):109–113.
86. Bugeon L, Danou A, Carpentier D, Langridge P, Syed N, Dallman MJ. Inducible gene silencing in podocytes: a new tool for studying glomerular function. *J Am Soc Nephrol.* 2003;14(3):786–791.
87. Liu JT, et al. Lipocalin-2 deficiency prevents endothelial dysfunction associated with dietary obesity: role of cytochrome P450 2C inhibition. *Br J Pharmacol.* 2012;165(2):520–531.
88. Li H, et al. Fibroblast growth factor 21 increases insulin sensitivity through specific expansion of subcutaneous fat. *Nat Commun.* 2018;9(1):272.
89. Rangan GK, Tesch GH. Quantification of renal pathology by image analysis. *Nephrology (Carlton).* 2007;12(6):553–558.
90. Fisher H, Hsu CY, Vittinghoff E, Lin F, Bansal N. Comparison of associations of urine protein-creatinine ratio versus albumin-creatinine ratio with complications of CKD: a cross-sectional analysis. *Am J Kidney Dis.* 2013;62(6):1102–1108.